

# INTEGRATING MULTIPLE RANDOM SKETCHES FOR SINGULAR VALUE DECOMPOSITION

TING-LI CHEN\*, DAWEI D. CHANG<sup>†</sup>, SU-YUN HUANG\*, HUNG CHEN<sup>†</sup>, CHIENYAO LIN\*, AND WEICHUNG WANG<sup>†</sup>

**Abstract.** The singular value decomposition (SVD) of large-scale matrices is a key tool in data analytics and scientific computing. The rapid growth in the size of matrices further increases the need for developing efficient large-scale SVD algorithms. Randomized SVD based on one-time sketching has been studied, and its potential has been demonstrated for computing a low-rank SVD. Instead of exploring different single random sketching techniques, we propose a Monte Carlo type integrated SVD algorithm based on multiple random sketches. The proposed integration algorithm takes multiple random sketches and then integrates the results obtained from the multiple sketched subspaces. So that the integrated SVD can achieve higher accuracy and lower stochastic variations. The main component of the integration is an optimization problem with a matrix Stiefel manifold constraint. The optimization problem is solved using Kolmogorov-Nagumo-type averages. Our theoretical analyses show that the singular vectors can be induced by population averaging and ensure the consistencies between the computed and true subspaces and singular vectors. Statistical analysis further proves a strong Law of Large Numbers and gives a rate of convergence by the Central Limit Theorem. Preliminary numerical results suggest that the proposed integrated SVD algorithm is promising.

**Key words.** low-rank singular value decomposition, randomized algorithm, integration of multiple random sketches, Stiefel manifold, Kolmogorov-Nagumo-type average, consistency of singular vectors.

**AMS subject classifications.** 65F15, 65C60, 68W20

**1. Introduction.** Singular value decomposition (SVD) of a matrix has been an essential tool in various theoretical studies and practical applications for decades. SVD has been studied in the fields of numerical linear algebra, applied mathematics, statistics, computer sciences, data analytics, physical sciences, engineering, and others. Its applications include imaging, medicine, social networks, signal processing, machine learning, information compression, and finance, just to name a few. In this article, we focus on low-rank SVD of a matrix, rather than the full SVD, which is sufficient in many scenarios. We concern the rank- $k$  SVD of a given  $m \times n$  real matrix

$$\mathbf{A} = \mathbf{U}\mathbf{\Sigma}\mathbf{V}^\top \approx \mathbf{U}_k \mathbf{\Sigma}_k \mathbf{V}_k^\top, \quad (1.1)$$

where  $\mathbf{U}\mathbf{\Sigma}\mathbf{V}^\top$  is the full SVD and  $\mathbf{U}_k \mathbf{\Sigma}_k \mathbf{V}_k^\top$  is the truncated rank- $k$  SVD. The columns of  $\mathbf{U}_k$  and  $\mathbf{V}_k$  are the  $k$  leading left and right singular vectors of  $\mathbf{A}$ , respectively. The diagonal entries of  $\mathbf{\Sigma}_k$  are the  $k$  largest singular values of  $\mathbf{A}$ .

The role of SVD in all types of applications remains vivid in the current big data era. However, as the size of data matrices generated or collected from simulations, experiments, detections, and observations continues to increase quickly, it is becoming a challenge to compute SVD for large matrices.

Randomized algorithms have been proposed and studied recently to find a rank- $k$  SVD of a large matrix. Such algorithms randomly project or sample from the underlying matrix  $\mathbf{A}$  to obtain a reduced matrix in a low-dimensional subspace. SVD

---

\*Institute of Statistical Science, Academia Sinica, Taipei 115, Taiwan (tlchen@stat.sinica.edu.tw, syhuang@stat.sinica.edu.tw, youyuoims94@gmail.com)

<sup>†</sup>Institute of Applied Mathematical Sciences, National Taiwan University, Taipei 106, Taiwan (davidzan830@gmail.com, hchen@math.ntu.edu.tw, send correspondence to wwang@ntu.edu.tw)

of this reduced matrix in low dimensions is performed and then mapped back to the original space to obtain an approximate SVD of  $\mathbf{A}$ . Several survey papers have reviewed the algorithms, computed error bounds, and numerical experiments in detail [4, 10, 14, 15, 25, 30]. Randomized SVD algorithms have been not only investigated theoretically but also used to solve problems such as large data set analysis [8], overdetermined least squares [18], partial differential equations [19], and inverse problems [27]. Randomized SVD is also used to solve linear system problems [20, 26] or act as a preconditioner [2, 3, 6, 7, 16]. Randomized SVD implementations built on top of MATLAB [21], parallel computers [1, 10, 29], and emerging architectures, such as GPUs [28], have appeared and continue to be improved.

Randomized SVD algorithms use a single random sketch and have demonstrated their advantages in various situations. In this article, we enhance randomized-type SVD by proposing a randomized SVD that integrates results obtained from multiple random sketches such that the integrated rank- $k$  SVD can achieve higher accuracy and less stochastic variations. Our discussion and analysis of this new algorithm include the following.

- We introduce a new way to compute rank- $k$  SVD based on multiple random sketches in Algorithm 2. Then, we develop two equivalent optimization problems (Theorem 2.2) with the Stiefel manifold constraint to integrate multiple subspace information sources from multiple random sketches. The proposed algorithm can be viewed as a Monte Carlo method that randomly samples many subspaces with an integration procedure based on averaging.
- To integrate the results obtained using multiple sketches, we propose Algorithm 3 to solve the constrained optimization problem iteratively and analyze its convergence behavior. In each iteration, the algorithm moves the current iterate using Kolmogorov-Nagumo-type averaging on top of the Stiefel manifold. The approach is motivated by averaging the independently identically distributed (i.i.d.) results from multiple sketches.
- The algorithm is analyzed statistically. In a key argument shown in Theorem 2.1, we assert that singular vectors can be induced by population averaging. This key theorem connects the two subspaces formed by the integration process and by the true singular vectors. Furthermore, based on this key theorem, we are able to prove the consistencies in terms of the subspace and singular vectors, the strong Law of Large Numbers, and the Central Limit Theorem for convergence rate.
- The numerical results, such as Figure 5.1, suggest that the integrated SVD can achieve higher accuracy and less stochastic variations using multiple random sketches.

This paper is organized as follows. We introduce the integrated SVD algorithm in Section 2, followed by a detailed discussion regarding how we integrate the multiple sketched results in Section 3. We analyze the algorithm statistically in Section 4. We present numerical results in Section 5. Finally, we conclude the paper in Section 6.

For the notations, we use lowercase letters or Greek letters for scalars (e.g.,  $m$ ,  $n$ , and  $\tau$ ), bold face letters for vectors (e.g.,  $\mathbf{x}$  and  $\mathbf{u}$ ), and bold face uppercase letters or bold face Greek letters for matrices (e.g.,  $\mathbf{A}$  and  $\mathbf{\Omega}$ ). We use  $\|\cdot\|_{\text{sp}}$  and  $\|\cdot\|_F$  to denote the matrix spectral norm and the matrix Frobenius norm, respectively. Table 1.1 summarizes the notations used in this article. We assume  $m \leq n$  here; however, all the algorithms and theoretical results can be applied to other cases.

$m, n$	Row and column dimensions of a matrix $\mathbf{A}$ with the assumption $m \leq n$
$k$	Desired rank of approximate SVD
$p$	Oversampling parameter
$\ell$	Dimension of randomized sketches, i.e., $\ell = (k + p) \ll n$
$q$	Exponent of the power method in Step 2 of Algorithms 1 and 2
$N$	Number of random sketches in Algorithm 2
$\mathbf{A} = \mathbf{U}\mathbf{\Sigma}\mathbf{V}^\top$	An $m \times n$ matrix and its SVD
$\mathbf{A} \approx \mathbf{U}_k \mathbf{\Sigma}_k \mathbf{V}_k^\top$	Rank- $k$ SVD defined in (1.1)
$\mathbf{A} \approx \tilde{\mathbf{U}}_k \tilde{\mathbf{\Sigma}}_k \tilde{\mathbf{V}}_k^\top$	Rank- $k$ SVD defined in (2.1) and computed by Algorithm 1 (rSVD)
$\mathbf{A} \approx \hat{\mathbf{U}}_k \hat{\mathbf{\Sigma}}_k \hat{\mathbf{V}}_k^\top$	Rank- $k$ SVD defined in (2.2) and computed by Algorithm 2 (iSVD)
$\mathbf{\Omega}$	A Gaussian random projection matrix in Algorithm 1
$\mathbf{\Omega}_{[i]}, i = 1 : N$	The $i$ th Gaussian random projection matrix in Algorithm 2
$\mathbf{Q}_{[i]}, i = 1 : N$	The $i$ th orthonormal basis of the sketched subspace in Algorithm 2
$\overline{\mathbf{Q}}$	The integrated orthonormal basis of the sketched subspace
$\overline{\mathbf{P}}$	The average of $\mathbf{Q}_{[i]} \mathbf{Q}_{[i]}^\top$ defined in (2.6) ( $\overline{\mathbf{P}}$ is simply for notation usage. It is not for computational purposes.)
$\mathcal{S}_{r,c}$	Matrix Stiefel manifold $\mathcal{S}_{r,c} := \{\mathbf{W} \in \mathbb{R}^{r \times c} : \mathbf{W}^\top \mathbf{W} = \mathbf{I}_c \text{ and } r \geq c\}$
$\mathcal{T}_{\mathbf{Q}} \mathcal{S}_{r,c}$	Tangent space of $\mathcal{S}_{r,c}$ at $\mathbf{Q}$
$\mathbf{Q}_c$	The current iterate for computing $\overline{\mathbf{Q}}$ in Algorithms 3
$\mathbf{Q}_+$	The updated iterate for computing $\overline{\mathbf{Q}}$ in Algorithms 3
$\mathbf{Q}, \mathbf{W}$	Points located on the matrix Stiefel manifold
$\mathbf{X}$	A point located on a tangent space
$F(\mathbf{Q})$	The objective function defined in (2.7) for computing $\overline{\mathbf{Q}}$
$\mathbf{G}_F(\mathbf{Q})$	Gradient of the objective function $F(\mathbf{Q})$
$\mathbf{D}_F(\mathbf{Q})$	Projected gradient onto the tangent space $\mathcal{T}_{\mathbf{Q}} \mathcal{S}_{m,\ell}$
$\varphi_{\mathbf{Q}}$	A lifting map to the tangent space in terms of $\mathbf{Q}$
$\varphi_{\mathbf{Q}}^{-1}$	A (specified version of) retraction map to the Stiefel manifold ( $\varphi_{\mathbf{Q}}$ and $\varphi_{\mathbf{Q}}^{-1}$ are associated with the Kolmogorov-Nagumo-type average.)

Table 1.1: Notations used in this article.

**2. Singular Value Decomposition via Multiple Random Sketches.** Randomized algorithms have been proposed to compute an approximate rank- $k$  SVD for matrices arising in various applications [10, 14, 25, 30]. The main idea of these algorithms is to (i) randomly project the matrix to a low-dimensional subspace, (ii) compute the SVD in this random subspace, and (iii) map this subspace SVD back to the original high-dimensional space. If the random sketch can capture most of the information regarding the largest  $k$  singular values and singular vectors, these algorithms can obtain satisfactory approximate rank- $k$  SVDs. We briefly review these randomized SVDs in Section 2.1.

To improve these randomized SVD algorithms based on a *single* sketch, it is natural to ask how we can find a better random subspace. Instead of exploring different single random sketching techniques, we propose a Monte Carlo integration method based on *multiple* random sketches in Section 2.2. The key idea is to repeat the process of random sketching multiple times. The multiple low-dimensional subspaces are then integrated. Based on this integrated subspace, we compute a rank- $k$  approximate SVD accordingly. By taking multiple random sketches, the resulting integrated

SVD is expected to have higher accuracy and smaller stochastic variation. On the other hand, the multiple sketches can be performed on parallel computers to reduce the execution time. Furthermore, the aforementioned multiple sketches lead to multiple low-dimensional random subspaces. We present an optimal representation of the multiple subspaces in Section 2.3, which is defined by a constrained optimization problem.

**2.1. Single Random Sketch.** Algorithm 1 is a common procedure for *randomized SVD* (rSVD) [9, 17] used to compute a rank- $k$  approximate SVD

$$\mathbf{A} \approx \tilde{\mathbf{U}}_k \tilde{\mathbf{\Sigma}}_k \tilde{\mathbf{V}}_k^\top. \quad (2.1)$$

The algorithm includes the following steps.

**Step 1.** The algorithm first generates a random matrix  $\mathbf{\Omega} \in \mathbb{R}^{n \times \ell}$ .

**Step 2.** The random matrix  $\mathbf{\Omega}$  is used to map the matrix  $\mathbf{A}$  to a low-dimensional subspace by  $\mathbf{Y} = (\mathbf{A}\mathbf{A}^\top)^q \mathbf{A}\mathbf{\Omega}$ . The  $q$ th power of the matrix  $\mathbf{A}\mathbf{A}^\top$  is applied here to improve the accuracy for the slow decay singular values [9, 24].

**Step 3.** Compute an orthonormal basis of  $\mathbf{Y}$  by, e.g., QR factorization or SVD so that the matrix  $\mathbf{Q}$  spans the randomized column subspace of  $\mathbf{A}\mathbf{\Omega}$ .

**Steps 4 and 5.** A smaller scale  $\ell \times n$  SVD and a matrix multiplication are performed to compute the SVD of the projected matrix in the column space of  $\mathbf{Q}$ . These two steps are equivalent to the operation  $\mathbf{Q}\mathbf{Q}^\top \mathbf{A} = \tilde{\mathbf{U}}_\ell \tilde{\mathbf{\Sigma}}_\ell \tilde{\mathbf{V}}_\ell^\top$ .

**Step 6.** Because the matrices  $\tilde{\mathbf{U}}_\ell$ ,  $\tilde{\mathbf{\Sigma}}_\ell$ , and  $\tilde{\mathbf{V}}_\ell$  contain over-sampled singular vectors and singular values, we extract the largest rank- $k$  approximate SVD including  $\tilde{\mathbf{U}}_k$ ,  $\tilde{\mathbf{\Sigma}}_k$ , and  $\tilde{\mathbf{V}}_k$  from these matrices.

---

**Algorithm 1** Randomized SVD with a single sketch (rSVD).

---

**Require:**  $\mathbf{A}$  (real  $m \times n$  matrix),  $k$  (desired rank of approximate SVD),  $p$  (oversampling parameter),  $\ell = k + p$  (dimension of the sketched column space),  $q$  (exponent of the power method)

**Ensure:** Approximate rank- $k$  SVD of  $\mathbf{A} \approx \tilde{\mathbf{U}}_k \tilde{\mathbf{\Sigma}}_k \tilde{\mathbf{V}}_k^\top$

- 1: Generate an  $n \times \ell$  random matrix  $\mathbf{\Omega}$
  - 2: Assign  $\mathbf{Y} \leftarrow (\mathbf{A}\mathbf{A}^\top)^q \mathbf{A}\mathbf{\Omega}$
  - 3: Compute  $\mathbf{Q}$  whose columns are an orthonormal basis of  $\mathbf{Y}$
  - 4: Compute the SVD of  $\mathbf{Q}^\top \mathbf{A} = \tilde{\mathbf{W}}_\ell \tilde{\mathbf{\Sigma}}_\ell \tilde{\mathbf{V}}_\ell^\top$
  - 5: Assign  $\tilde{\mathbf{U}}_\ell \leftarrow \mathbf{Q}\tilde{\mathbf{W}}_\ell$
  - 6: Extract the largest  $k$  singular-pairs from  $\tilde{\mathbf{U}}_\ell$ ,  $\tilde{\mathbf{\Sigma}}_\ell$ ,  $\tilde{\mathbf{V}}_\ell$  to obtain  $\tilde{\mathbf{U}}_k$ ,  $\tilde{\mathbf{\Sigma}}_k$ ,  $\tilde{\mathbf{V}}_k$  in (2.1)
- 

**2.2. Multiple Random Sketches.** The rSVD (Algorithm 1) maps the matrix  $\mathbf{A}$  onto a low-dimensional subspace using a *single* random sketch. We extend the rSVD by proposing an integrated singular value decomposition (iSVD), which uses *multiple* sketches. The procedure of iSVD is outlined in Algorithm 2. In addition to those input parameters listed in rSVD, the proposed iSVD (Algorithm 2) takes an extra parameter: the number of random sketches  $N$ . In return, iSVD outputs the integrated approximate rank- $k$  SVD

$$\mathbf{A} \approx \hat{\mathbf{U}}_k \hat{\mathbf{\Sigma}}_k \hat{\mathbf{V}}_k^\top. \quad (2.2)$$

In Steps 1, 2, and 3 of Algorithm 2, iSVD performs multiple sketches by repeating the sketching process described in the first three steps of the rSVD algorithm  $N$

---

**Algorithm 2** Integrated SVD with multiple sketches (iSVD).

---

**Require:**  $\mathbf{A}$  (real  $m \times n$  matrix),  $k$  (desired rank of approximate SVD),  $p$  (oversampling parameter),  $\ell = k + p$  (dimension of the sketched column space),  $q$  (exponent of the power method),  $N$  (number of random sketches)

**Ensure:** Approximate rank- $k$  SVD of  $\mathbf{A} \approx \widehat{\mathbf{U}}_k \widehat{\mathbf{\Sigma}}_k \widehat{\mathbf{V}}_k^\top$

- 1: Generate  $n \times \ell$  random matrices  $\mathbf{\Omega}_{[i]}$  for  $i = 1, \dots, N$
  - 2: Assign  $\mathbf{Y}_{[i]} \leftarrow (\mathbf{A}\mathbf{A}^\top)^q \mathbf{A}\mathbf{\Omega}_{[i]}$  for  $i = 1, \dots, N$  (in parallel)
  - 3: Compute  $\mathbf{Q}_{[i]}$  whose columns are an orthonormal basis of  $\mathbf{Y}_{[i]}$  (in parallel)
  - 4: Integrate  $\overline{\mathbf{Q}} \leftarrow \{\mathbf{Q}_{[i]}\}_{i=1}^N$  (by Algorithm 3)
  - 5: Compute the SVD of  $\overline{\mathbf{Q}}^\top \mathbf{A} = \widehat{\mathbf{W}}_\ell \widehat{\mathbf{\Sigma}}_\ell \widehat{\mathbf{V}}_\ell^\top$
  - 6: Assign  $\widehat{\mathbf{U}}_\ell \leftarrow \overline{\mathbf{Q}} \widehat{\mathbf{W}}_\ell$
  - 7: Extract the largest  $k$  singular pairs from  $\widehat{\mathbf{U}}_\ell, \widehat{\mathbf{\Sigma}}_\ell, \widehat{\mathbf{V}}_\ell$  to obtain  $\widehat{\mathbf{U}}_k, \widehat{\mathbf{\Sigma}}_k, \widehat{\mathbf{V}}_k$  in (2.2)
- 

times. In Step 4, the multiple orthonormal basis matrices  $\mathbf{Q}_{[i]}$  are integrated. Using the integrated orthonormal basis matrix  $\overline{\mathbf{Q}}$ , we can obtain an approximate SVD by Steps 5, 6, and 7. Note that, in Step 1 of the two algorithms, we consider Gaussian random projection matrices  $\mathbf{\Omega}$  in rSVD and  $\mathbf{\Omega}_{[i]}$  in iSVD. Either  $\mathbf{\Omega}$  or  $\mathbf{\Omega}_{[i]}$  is an  $n \times \ell$  random matrix whereby each of the entries is i.i.d. standard Gaussian. The matrix  $\mathbf{A}\mathbf{\Omega}$  (or  $\mathbf{A}\mathbf{\Omega}_{[i]}$ ) is a random mapping from  $\mathbb{R}^{m \times n}$  to a low-dimensional subspace  $\mathbf{Y}$  (or  $\mathbf{Y}_{[i]}) \in \mathbb{R}^{m \times \ell}$  with  $\ell \ll n$ . Furthermore, each of the columns in  $\mathbf{A}\mathbf{\Omega}$  (or  $\mathbf{A}\mathbf{\Omega}_{[i]}$ ) is a linear combination of the columns of  $\mathbf{A}$  with random Gaussian mixing coefficients.

We use a simple example to illustrate the ideas of iSVD. Let  $\mathbf{A} = \text{diag}([25, 5, 1])$  be a diagonal  $3 \times 3$  matrix. We have the (true) SVD of  $\mathbf{A} = \mathbf{U}\mathbf{\Sigma}\mathbf{U}^\top$ , where  $\mathbf{U}$  is the  $3 \times 3$  identity matrix and  $\mathbf{\Sigma} = \text{diag}([25, 5, 1])$ . As shown in Parts (a) and (b) of Figure 2.1, we randomly project  $\mathbf{A}$  onto  $\mathbb{R}^{3 \times 1}$  by letting  $\mathbf{\Omega}_{[i]} \in \mathbb{R}^{3 \times 1}$  with  $q = 0$  and  $N = 2, 5$ . The bases of the projected subspaces  $\mathbf{Q}_{[i]} \in \mathbb{R}^{3 \times 1}$  are shown by the green vectors, and the integrated basis  $\overline{\mathbf{Q}}$  is shown as the red vector. It is clear that the  $\overline{\mathbf{Q}}$  corresponding to  $N = 5$  is more close to the first singular vector  $[1, 0, 0]$ . Consequently, we can obtain more accurate SVD  $\widehat{\mathbf{U}}_k \widehat{\mathbf{\Sigma}}_k \widehat{\mathbf{V}}_k^\top$  by iSVD over the subspace  $\overline{\mathbf{Q}}$ . In Parts (c) and (d), we show similar results obtained by letting  $\mathbf{\Omega}_{[i]} \in \mathbb{R}^{3 \times 2}$ . The  $\overline{\mathbf{Q}}$  is more close to the 2-dimensional subspace spanned by the first two singular vectors  $[1, 0, 0]$  and  $[0, 1, 0]$  using larger  $N$ .

We have proposed the iSVD algorithm based on multiple random sketches in Section 2.2. Obviously, the key component of iSVD is the integration process in Step 4 of Algorithm 2. This is the focus of the next section.

### 2.3. An Optimal Representation of the Multiple Projected Subspaces.

The integration process in Step 4 of Algorithm 2 finds a matrix  $\overline{\mathbf{Q}}$  that “best” represents the matrices  $\mathbf{Q}_{[i]}$  for  $i = 1, \dots, N$ . In other words, because each  $\mathbf{Q}_{[i]}$  contains the orthonormal basis of the randomly projected subspace  $\mathbf{Y}_{[i]}$ , the process intends to integrate these  $N$  randomly projected subspaces into a single subspace spanned by the columns of  $\overline{\mathbf{Q}}$ . Consequently, this integrated subspace contains as much information of the leading left singular vectors as possible. Then, in Steps 5 and 6 of Algorithm 2, we compute the SVD in  $\overline{\mathbf{Q}}\overline{\mathbf{Q}}^\top \mathbf{A}$ , which is the low-dimensional projection of  $\mathbf{A}$  onto the subspace spanned by the columns of  $\overline{\mathbf{Q}}$ . In particular, we define

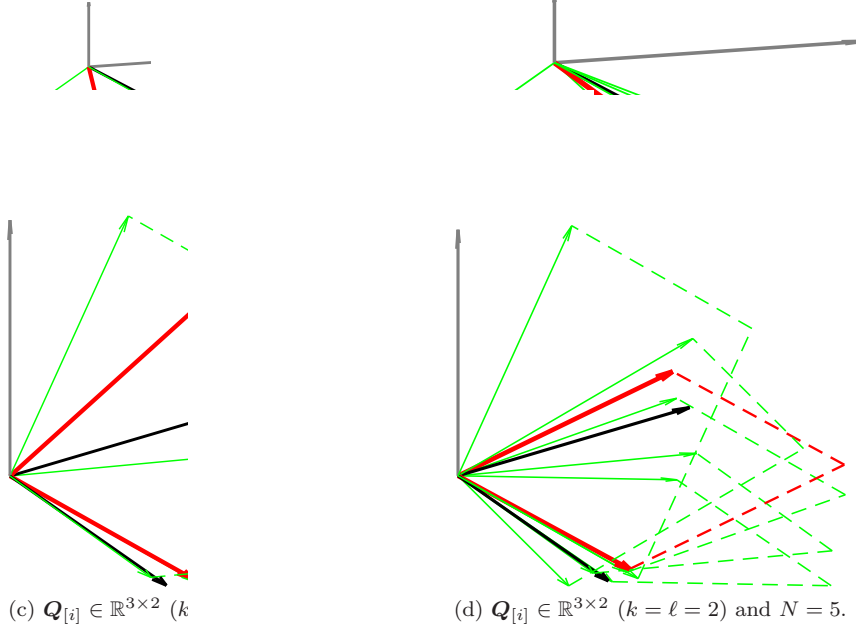


Fig. 2.1: The orthonormal bases of randomly projected 1-dimensional subspaces  $\mathbf{Q}_{[i]}$ ,  $i = 1, \dots, N$ , are plotted (in green) for (a)  $N = 2$  and (b)  $N = 5$ . The basis of the integrated subspace  $\overline{\mathbf{Q}}$  (in red) is closer to the first singular vector  $[1, 0, 0]$  for  $N = 5$ . Similar plots on 2-dimensional subspaces are plotted for (c)  $N = 2$  and (d)  $N = 5$ . The 2-dimensional subspace spanned by  $\overline{\mathbf{Q}}$  is closer to the subspace spanned by the first two singular vectors for  $N = 5$ .

such best representation  $\overline{\mathbf{Q}}$  by solving the following optimization problem:

$$\overline{\mathbf{Q}} := \operatorname{argmin}_{\mathbf{Q} \in \mathcal{S}_{m, \ell}} \sum_{i=1}^N \left\| \mathbf{Q}_{[i]} \mathbf{Q}_{[i]}^\top - \mathbf{Q} \mathbf{Q}^\top \right\|_F^2. \quad (2.3)$$

The matrix  $\overline{\mathbf{Q}}$  is constrained on the matrix Stiefel manifold because the columns of  $\overline{\mathbf{Q}}$  form the orthonormal basis of the integrated subspace. Next, we justify this definition of the  $\overline{\mathbf{Q}}$  from the viewpoints of geometry and stochastic expectation.

This definition of  $\overline{\mathbf{Q}}$  has its geometrical motivations. At first glance, we can average the  $\mathbf{Q}_{[i]}$  by computing  $\mathbf{Q}_{ave} = \frac{1}{N} \sum_{i=1}^N \mathbf{Q}_{[i]}$  and then orthonormalize the columns of  $\mathbf{Q}_{ave}$  to obtain an average representation of  $\mathbf{Q}_{[i]}$ . However, this simple averaging scheme can be misguided. For example, let  $\mathbf{Q}_{[1]} = [\mathbf{q}_1, \mathbf{q}_2]$  and  $\mathbf{Q}_{[2]} = [\mathbf{q}_2, \mathbf{q}_1]$  be two equivalent matrices with respect to an orthogonal transformation. The simple averaging scheme suggests that  $\mathbf{Q}_{ave} = \frac{1}{2}[\mathbf{q}_1 + \mathbf{q}_2, \mathbf{q}_1 + \mathbf{q}_2]$ , which is rank deficient. Fortunately, we observe that the equivalence of  $\mathbf{Q}_{[1]}$  and  $\mathbf{Q}_{[2]}$  can be revealed by the equation  $\mathbf{Q}_{[1]} \mathbf{Q}_{[1]}^\top = \mathbf{Q}_{[2]} \mathbf{Q}_{[2]}^\top$ . On the other hand, in general, any orthogonal transformation on the right-hand side of  $\mathbf{Q}_{[i]}$  can be represented by  $\mathbf{Q}_{[i]} \mathbf{R}$ , where  $\mathbf{R}$  is an orthogonal matrix. The fact that  $(\mathbf{Q}_{[i]} \mathbf{R})(\mathbf{Q}_{[i]} \mathbf{R})^\top = \mathbf{Q}_{[i]} \mathbf{Q}_{[i]}^\top$  suggests that the matrices  $\mathbf{Q}_{[i]}$  and  $\mathbf{Q}_{[i]} \mathbf{R}$  are equivalent in the sense that they span the same column subspace. These geometric observations partially motivate us to define the integrated orthonormal matrix  $\overline{\mathbf{Q}}$  shown in (2.3).

Furthermore, we emphasize another important reason why we focus on the projection matrices  $\mathbf{Q}_{[i]}\mathbf{Q}_{[i]}^\top$  by presenting the following key Theorem 2.1. The theorem suggests that the population average of the projection matrices  $E(\mathbf{Q}_{[i]}\mathbf{Q}_{[i]}^\top)$  can reveal the *true* left singular vectors of  $\mathbf{A}$ . Furthermore, in Section 4, we will apply Theorem 2.1 to show the Strong Law of Large Numbers, the consistency of the singular vectors, and the Central Limit Theorem for iSVD. The proof of Theorem 2.1 can be found in Appendix A.1.

THEOREM 2.1 (Singular vectors induced by population averaging). *Let  $\mathbf{Q}_{[i]}$  be the orthonormal basis of the  $i$ th random subspace computed by Algorithm 2 with  $\Omega_{[i]}$  having i.i.d. Gaussian entries. At the population level, the expected arithmetic mean of these projection matrices has the property of having the same left singular vectors as the matrix  $\mathbf{A}$ . Specifically,*

$$E(\mathbf{Q}_{[i]}\mathbf{Q}_{[i]}^\top) = \mathbf{U}\mathbf{\Lambda}\mathbf{U}^\top. \quad (2.4)$$

Here,  $\mathbf{U}$  consists of left singular vectors of  $\mathbf{A}$ , as shown in (1.1). For  $\mathbf{\Lambda}$  defined in (A.1), we can show that (a)  $\mathbf{\Lambda}$  is a diagonal matrix, (b) each of the diagonal entries belongs to  $(0, 1)$ , and (c) these diagonal entries are strictly decreasing if the underlying matrix  $\mathbf{A}$  has strictly decreasing singular values.

It is worth noting that we can regard  $E(\mathbf{Q}_{[i]}\mathbf{Q}_{[i]}^\top)$  as the limiting case of taking an average over infinitely many projection matrices:  $E(\mathbf{Q}_{[i]}\mathbf{Q}_{[i]}^\top) = \lim_{N \rightarrow \infty} \overline{\mathbf{P}}$ , where

$$\overline{\mathbf{P}} := \frac{1}{N} \sum_{i=1}^N \mathbf{Q}_{[i]}\mathbf{Q}_{[i]}^\top \quad (2.5)$$

is the empirical arithmetic average of the  $N$  projection matrices. The theorem suggests the following essential property. Even a projection matrix  $\mathbf{Q}_{[i]}\mathbf{Q}_{[i]}^\top$  is associated with a low-dimensional (rank- $\ell$ ) subspace only, the arithmetic average  $\overline{\mathbf{P}}$  contains not only information of the leading rank- $\ell$  subspace but also information for other subspaces spanned by *all true* singular vectors if the number of random sketches  $N$  is sufficiently large. Furthermore, because the entries of  $\mathbf{\Lambda}$  are strictly decreasing, the columns of  $\mathbf{U}$  match the left singular vectors in a correct order. The following example illustrates the property given in Theorem 2.1. Let  $\mathbf{A} = \text{diag}([25, 5, 1, 0.2])$  be a diagonal  $4 \times 4$  matrix. Then, we have the true SVD of  $\mathbf{A} = \mathbf{U}\mathbf{\Sigma}\mathbf{U}^\top$ , where  $\mathbf{U}$  is the  $4 \times 4$  identity matrix and  $\mathbf{\Sigma} = \text{diag}([25, 5, 1, 0.2])$ . By computing the SVD of  $\overline{\mathbf{P}} \in \mathbb{R}^{4 \times 4}$  with a set of  $\mathbf{Q}_{[i]} \in \mathbb{R}^{4 \times 2}$  (i.e., the dimension of the random sketches  $\ell = 2$ ), we obtain the following estimations of

$$\mathbf{U} \approx \begin{bmatrix} -1.00 & .021 & -.004 & .010 \\ -.021 & -.998 & -.044 & -.046 \\ .004 & .046 & -.998 & -.036 \\ .009 & -.044 & -.038 & .998 \end{bmatrix} \quad \text{and} \quad \begin{bmatrix} -1.00 & -.020 & .002 & .004 \\ .020 & -1.00 & -.003 & -.009 \\ -.002 & .003 & -1.00 & -.001 \\ .004 & -.009 & -.001 & 1.00 \end{bmatrix},$$

for  $N = 10$  and  $N = 100$ , respectively. The corresponding estimations of  $\mathbf{\Lambda} \approx \text{diag}([.997, .848, .149, .006])$  and  $\text{diag}([.992, .819, .177, .012])$ . The approximate  $\mathbf{U}$  for  $N = 100$  is much closer to the whole true  $\mathbf{U}$  even though the dimension of the random sketches is 2, rather than the dimension of the matrix, which is 4.

Although Equation (2.4) reveals important insight into the average of the  $\mathbf{Q}_{[i]}\mathbf{Q}_{[i]}^\top$ , the equation has its limits from the perspective of numerical computation. First, we cannot compute the true singular values  $\mathbf{\Sigma}$  and the right singular vectors  $\mathbf{V}$  using

Equation (2.4). Second, the diagonal entries of  $\mathbf{A}$  are clustered in the interval  $(0, 1)$ , and such clustering may affect the accuracy of the computed  $\mathbf{U}$ . These difficulties can be overcome by considering another optimization problem shown in Theorem 2.2.

In Theorem 2.2, we present two alternative optimization problems that are equivalent to the optimization problem (2.3). The first equivalent optimization problem is shown in (2.6). In this formulation, we apply the concept of (2.4) to compute  $\overline{\mathbf{Q}}$ . The second equivalent formulation is shown in (2.7), which is defined by a differentiable objective function. We will develop an algorithm to solve this problem in Section 3. This decision is based on the following two reasons. The dimension of  $\mathbf{Q}_{[i]}\mathbf{Q}_{[i]}^\top$  in (2.6) ( $m \times m$ ) can be much larger than the dimension of the matrix  $\mathbf{Q}^\top \overline{\mathbf{P}}\mathbf{Q}$  in (2.7) ( $\ell \times \ell$ ). Furthermore, the objective function  $F(\mathbf{Q})$  is differentiable, which allows us to develop algorithms to solve the optimization problem based on the gradient of  $F(\mathbf{Q})$ . The proof of Theorem 2.2 can be found in Appendix A.2.

**THEOREM 2.2** (Equivalent optimization problems). *The minimization problem (2.3) is equivalent to the following two optimization problems:*

$$(i) \quad \overline{\mathbf{Q}} := \operatorname{argmin}_{\mathbf{Q} \in \mathcal{S}_{m,\ell}} \|\overline{\mathbf{P}} - \mathbf{Q}\mathbf{Q}^\top\|_F^2 \quad (2.6)$$

and

$$(ii) \quad \overline{\mathbf{Q}} := \operatorname{argmax}_{\mathbf{Q} \in \mathcal{S}_{m,\ell}} F(\mathbf{Q}), \quad (2.7)$$

where  $\overline{\mathbf{P}}$  is defined in (2.5) and  $F(\mathbf{Q}) = \frac{1}{2} \operatorname{tr}(\mathbf{Q}^\top \overline{\mathbf{P}}\mathbf{Q})$  is a differential function. These equivalences are up to an orthogonal matrix multiplied on the right-hand side of  $\overline{\mathbf{Q}}$ .

In short, in Step 4 of Algorithm 2, we need to integrate the orthogonal matrices  $\mathbf{Q}_{[i]}$  into one orthogonal matrix  $\overline{\mathbf{Q}} \in \mathbb{R}^{m \times \ell}$  that “best” represents these matrices. We propose using the particular  $\overline{\mathbf{Q}}$  defined by the Stiefel-manifold-constrained optimization problem (2.7). In the next section, we will discuss how we compute  $\overline{\mathbf{Q}}$  by an iterative method based on the Kolmogorov-Nagumo-type average. In Section 4, we will prove that this optimal representation  $\overline{\mathbf{Q}}$  converges to the best rank- $\ell$  approximation with probability one when the number of sketches  $N$  tends to infinity.

**3. Integration of Sketched Subspaces.** The goal of this section is to develop an iterative method based on a Kolmogorov-Nagumo-type average to compute  $\overline{\mathbf{Q}}$  by solving the constrained optimization (2.7). We start the development of the integration algorithm by introducing some background in Section 3.1. This background includes the Kolmogorov-Nagumo-type average of sample points on a matrix Stiefel manifold and derives the gradients of the objective function. Because a Kolmogorov-Nagumo-type average is defined by a lifting map and a corresponding retraction map, we derive a particular lifting and retraction map pair that can be applied to solve the constrained optimization (2.7) in Sections 3.2 and 3.3. Based on the lifting and retraction maps, we propose the integration algorithm in Section 3.4. The convergence analysis and some remarks on the algorithm are given in Section 3.5.

**3.1. Background.** We introduce the Kolmogorov-Nagumo-type average and derive the gradient of the objective function that will be used to integrate the sketched subspaces by solving the optimization problem (2.7).

First, we introduce the Kolmogorov-Nagumo-type average. Taking an average is the most commonly used summary statistic for independently and identically distributed (i.i.d.) data. The orthogonal matrices  $\{\mathbf{Q}_{[i]}\}_{i=1}^N$  from repeated runs of



random sketches are independently obtained from a common stochastic randomization mechanism and thus are i.i.d. The integration of multiple random sketches can be seen as an ‘‘average’’ of these orthogonal matrices. However, it is no longer in the traditional sense of taking an average in a Euclidean space; rather, it is a Kolmogorov-Nagumo-type average defined in (3.1). A Kolmogorov-Nagumo-type average of  $\{\boldsymbol{\mu}_i\}_{i=1}^N$  is defined as

$$\bar{\boldsymbol{\mu}}_{KN} = \varphi^{-1} \left( \frac{1}{N} \sum_{i=1}^N \varphi(\boldsymbol{\mu}_i) \right), \quad (3.1)$$

where  $\varphi$  is a continuous and locally one-to-one lifting map and  $\varphi^{-1}$  is the paired retraction map. Note that the traditional arithmetic average can be defined by letting  $\varphi$  and  $\varphi^{-1}$  be the identity maps, and the geometric average of positive numbers can be defined by letting  $\varphi$  be the logarithm function and  $\varphi^{-1}$  be the exponential function. In our integration algorithm, we consider the case in which  $\boldsymbol{\mu}_i = \mathbf{Q}_{[i]}$  and use the notation  $\varphi_{\mathbf{Q}}$  and  $\varphi_{\mathbf{Q}}^{-1}$  to emphasize that the lifting and retraction maps depend on a given  $\mathbf{Q} \in \mathcal{S}_{m,\ell}$ . In the next two sections, we derive a lifting map  $\varphi_{\mathbf{Q}} : \mathcal{S}_{m,\ell} \rightarrow \mathcal{T}_{\mathbf{Q}}\mathcal{S}_{m,\ell}$  and its corresponding retraction map  $\varphi_{\mathbf{Q}}^{-1} : \mathcal{T}_{\mathbf{Q}}\mathcal{S}_{m,\ell} \rightarrow \mathcal{S}_{m,\ell}$ , which satisfy certain properties for solving the optimization problem (2.7). Various Kolmogorov-Nagumo-type averages of sample points on a Stiefel manifold can be found in [5, 11].

Second, we address the (projected) gradient of  $F(\mathbf{Q})$ . Many optimization schemes, including the scheme to be proposed in Section 3, require the derivatives of the objective function. Theorem 2.2 has asserted that (2.3) is equivalent to the problem (2.7) with a differentiable objective function  $F(\mathbf{Q})$ . We further present Theorem 3.1 to show how we can compute the gradient ascent direction of  $F(\mathbf{Q})$  at a certain  $\mathbf{Q} \in \mathbb{R}^{m \times \ell}$  by (3.2) and show how we can project the gradient ascent direction to the tangent space of  $\mathcal{S}_{m,\ell}$  at  $\mathbf{Q}$  (denoted as  $\mathcal{T}_{\mathbf{Q}}\mathcal{S}_{m,\ell}$ ), as shown in (3.3). See Appendix A.3 for the proof of Theorem 3.1.

**THEOREM 3.1.** *Let  $\mathbf{G}_F(\mathbf{Q})$  denote the gradient (the usual derivative in the Euclidean space) of  $F(\mathbf{Q})$  with respect to  $\mathbf{Q} \in \mathbb{R}^{m \times \ell}$ , and let  $\mathbf{D}_F(\mathbf{Q})$  denote the projected gradient of  $\mathbf{G}_F(\mathbf{Q})$  onto the tangent space  $\mathcal{T}_{\mathbf{Q}}\mathcal{S}_{m,\ell}$ . We have*

$$\mathbf{G}_F(\mathbf{Q}) := \left[ \frac{\partial F(\mathbf{Q})}{\partial \mathbf{Q}} \right] = \bar{\mathbf{P}}\mathbf{Q} \in \mathbb{R}^{m \times \ell}, \quad (3.2)$$

where  $\bar{\mathbf{P}}$  is defined in (2.5), and

$$\mathbf{D}_F(\mathbf{Q}) := \Pi_{\mathcal{T}_{\mathbf{Q}}}\mathbf{G}_F(\mathbf{Q}) = (\mathbf{I}_m - \mathbf{Q}\mathbf{Q}^\top)\mathbf{G}_F(\mathbf{Q}), \quad (3.3)$$

where  $\Pi_{\mathcal{T}_{\mathbf{Q}}}$  is the projection from  $\mathbb{R}^{m \times \ell}$  to  $\mathcal{T}_{\mathbf{Q}}\mathcal{S}_{m,\ell}$ .

**3.2. The Lifting Map.** For a given  $\mathbf{Q} \in \mathcal{S}_{m,\ell}$ , we define the lifting map

$$\varphi_{\mathbf{Q}}(\mathbf{W}) = (\mathbf{I}_m - \mathbf{Q}\mathbf{Q}^\top)\mathbf{W}\mathbf{W}^\top\mathbf{Q} : \mathcal{S}_{m,\ell} \rightarrow \mathcal{T}_{\mathbf{Q}}\mathcal{S}_{m,\ell} \quad (3.4)$$

for any  $\mathbf{W} \in \mathcal{S}_{m,\ell}$ . Our definition of  $\varphi$  leads to an important property:

$$\frac{1}{N} \sum_{i=1}^N \varphi_{\mathbf{Q}_c}(\mathbf{Q}_{[i]}) = \mathbf{D}_F(\mathbf{Q}_c), \quad (3.5)$$

where  $\mathbf{Q}_c$  denotes the current iterate. Specifically, the average of the mapped points  $\varphi_{\mathbf{Q}_c}(\mathbf{Q}_{[i]})$  on the tangent space of the current iterate is simply the projected gradient

at this current iterate. This property links the Kolmogorov-Nagumo-type average to the gradient ascent method for the optimal representation in (2.3) and its equivalent formulation in (2.7). If the projected gradient  $\mathbf{D}_F(\mathbf{Q}_c)$  is zero (or numerically close to zero), then  $\mathbf{Q}_c$  has reached a stationary point for the optimization problem (2.7). If it is not zero, we search for the next iterate along the path  $\mathcal{Q}(\tau) := \varphi_{\mathbf{Q}_c}^{-1}(\tau \mathbf{D}_F(\mathbf{Q}_c))$  on the manifold, where  $\tau > 0$  is a step size. In the Kolmogorov-Nagumo-type average, we take  $\tau = 1$  for simplicity. Because  $\varphi_{\mathbf{Q}_c}$  is only locally one to one, we need to specify a version of the retraction map  $\varphi_{\mathbf{Q}_c}^{-1}$  to pull points on  $\mathcal{T}_{\mathbf{Q}_c} \mathcal{S}_{m,\ell}$  back to  $\mathcal{S}_{m,\ell}$ . Below, we discuss the derivation of a proper version of  $\varphi_{\mathbf{Q}_c}^{-1}$ .

**3.3. The Retraction Map.** Next, we derive the corresponding retraction map  $\varphi_{\mathbf{Q}}^{-1} : \mathcal{T}_{\mathbf{Q}} \mathcal{S}_{m,\ell} \rightarrow \mathcal{S}_{m,\ell}$ . For  $\mathbf{W} \in \mathcal{S}_{m,\ell}$ , we can express it as  $\mathbf{W} = \mathbf{Q}\mathbf{C} + \mathbf{Q}_{\perp}\mathbf{B}$ , where  $\mathbf{Q}_{\perp}^{\top} \mathbf{Q}_{\perp} = \mathbf{I}_{m-\ell}$  and  $\mathbf{Q}^{\top} \mathbf{Q}_{\perp} = \mathbf{0}$ . Without loss of generality, we may assume that  $\mathbf{C}$  is symmetric. If not, we can find an orthogonal matrix  $\mathbf{R}$  such that  $\mathbf{C}\mathbf{R}$  is symmetric. Because  $(\mathbf{W}\mathbf{R})(\mathbf{W}\mathbf{R})^{\top} = \mathbf{W}\mathbf{W}^{\top}$  for any orthogonal matrix  $\mathbf{R}$ , we treat  $\mathbf{W}$  and  $\mathbf{W}\mathbf{R}$  as equivalent. Next, we present two lemmas that will be used in deriving  $\varphi_{\mathbf{Q}}^{-1}(\mathbf{X})$ , where  $\mathbf{X} \in \mathcal{T}_{\mathbf{Q}} \mathcal{S}_{m,\ell}$ . The proofs are given in Appendices A.4 and A.5.

LEMMA 3.2. *For a given  $\mathbf{Q} \in \mathcal{S}_{m,\ell}$ , we have the following properties. (a) The matrix  $\frac{\mathbf{I}_{\ell}}{4} - \varphi_{\mathbf{Q}}(\mathbf{W})^{\top} \varphi_{\mathbf{Q}}(\mathbf{W})$  is non-negative definite for any arbitrary  $\mathbf{W} \in \mathcal{S}_{m,\ell}$ . (b) Let  $\mathbf{X} = \frac{1}{N} \sum_{i=1}^N \varphi_{\mathbf{Q}}(\mathbf{Q}_{[i]})$ . Then,  $\frac{\mathbf{I}_{\ell}}{4} - \mathbf{X}^{\top} \mathbf{X}$  is non-negative definite.*

LEMMA 3.3. *For a given  $\mathbf{X} \in \mathcal{T}_{\mathbf{Q}} \mathcal{S}_{m,\ell}$  that satisfies the conditions  $\mathbf{Q}^{\top} \mathbf{X} = \mathbf{0}$  and  $\frac{\mathbf{I}_{\ell}}{4} - \mathbf{X}^{\top} \mathbf{X}$  being non-negative definite, there exists a  $\mathbf{W} \in \mathcal{S}_{m,\ell}$  such that  $\varphi_{\mathbf{Q}}(\mathbf{W}) = \mathbf{X}$ . Furthermore, if  $\mathbf{W}$  is restricted to the column span of  $\mathbf{Q}$  and  $\mathbf{X}$ , i.e.,*

$$\mathbf{W} \in \{\mathbf{W} \in \mathcal{S}_{m,\ell} : \mathbf{W} = \mathbf{Q}\mathbf{C} + \mathbf{X}\mathbf{B}, \mathbf{C} \text{ symmetric}\},$$

then, up to an orthogonal transformation on the right side,  $\mathbf{W}$  has to take the following form  $\mathbf{W} = \mathbf{Q}\mathbf{C} + \mathbf{X}\mathbf{C}^{-1}$ , where  $\mathbf{C} = \left\{ \frac{\mathbf{I}_{\ell}}{2} + \left( \frac{\mathbf{I}_{\ell}}{4} - \mathbf{X}^{\top} \mathbf{X} \right)^{1/2} \right\}^{1/2}$  and the matrix square root is defined in Appendix A.6.

Because the matrix square root is not unique, Lemma 3.3 presents many possible choices of  $\mathbf{W}$  as a pre-image for  $\mathbf{X}$  such that  $\varphi_{\mathbf{Q}}(\mathbf{W}) = \mathbf{X}$ . Here, we will confine the matrix square root involved in  $\mathbf{C}$  to be symmetric and non-negative definite so that the inverse map  $\varphi_{\mathbf{Q}}^{-1}(\mathbf{X}) = \mathbf{Q}\mathbf{C} + \mathbf{X}\mathbf{C}^{-1}$  is uniquely specified. Furthermore, if  $\mathbf{X} \in \mathcal{T}_{\mathbf{Q}} \mathcal{S}_{m,\ell}$  satisfies the condition that  $\frac{\mathbf{I}_{\ell}}{4} - \mathbf{X}^{\top} \mathbf{X}$  is non-negative definite, then  $\frac{\mathbf{I}_{\ell}}{4} - (\tau \mathbf{X}^{\top})(\tau \mathbf{X})$  is also non-negative definite for any  $\tau \in [0, 1]$ . Thus, we can extend Lemma 3.3 to obtain a unique path on the manifold, wherein all matrix square roots involved are taken to be symmetric and non-negative definite.

THEOREM 3.4 (Retraction Map). *For a given  $\mathbf{X} \in \mathcal{T}_{\mathbf{Q}} \mathcal{S}_{m,\ell}$  that satisfies the conditions  $\mathbf{Q}^{\top} \mathbf{X} = \mathbf{0}$  and  $\frac{\mathbf{I}_{\ell}}{4} - \mathbf{X}^{\top} \mathbf{X}$  being non-negative definite, there exists a path  $\mathcal{Q}(\tau) \in \mathcal{S}_{m,\ell}$  for  $\tau \in [0, 1]$  such that  $\varphi_{\mathbf{Q}}(\mathcal{Q}(\tau)) = \tau \mathbf{X}$  and the retraction map is given by*

$$\varphi_{\mathbf{Q}}^{-1}(\tau \mathbf{X}) = \mathbf{Q}\mathbf{C} + \tau \mathbf{X}\mathbf{C}^{-1}, \quad (3.6)$$

where

$$\mathbf{C} = \left\{ \frac{\mathbf{I}_{\ell}}{2} + \left( \frac{\mathbf{I}_{\ell}}{4} - \tau^2 \mathbf{X}^{\top} \mathbf{X} \right)^{1/2} \right\}^{1/2} \quad (3.7)$$

with all matrix square roots taken to be symmetric and non-negative definite.

**3.4. The Integration Algorithm.** Now, we are ready to propose Algorithm 3, which solves the optimization problem (2.7) to find  $\overline{\mathbf{Q}}$  by iteratively updating the Kolmogorov-Nagumo-type averages. The inputs of Algorithm 3 are the matrices  $\{\mathbf{Q}_{[i]}\}_{i=1}^N \in \mathcal{S}_{m,\ell}$  and an initial iterate  $\mathbf{Q}_{\text{ini}}$ . The output of the algorithm is the (approximate) integrated  $\overline{\mathbf{Q}}$  defined in (2.7).

---

**Algorithm 3** Integration of  $\{\mathbf{Q}_{[i]}\}_{i=1}^N$  based on the Kolmogorov-Nagumo-type average.

---

**Require:**  $\mathbf{Q}_{[1]}, \mathbf{Q}_{[2]}, \dots, \mathbf{Q}_{[N]}, \mathbf{Q}_{\text{ini}}$

**Ensure:** Integrated  $\overline{\mathbf{Q}}$  defined in (2.7)

- 1: Initialize the current iterate  $\mathbf{Q}_c \leftarrow \mathbf{Q}_{\text{ini}}$
  - 2: **while** (not convergent) **do**
  - 3:   Compute  $\varphi_{\mathbf{Q}_c}(\mathbf{Q}_{[i]})$  defined in (3.9) by lifting and averaging
  - 4:   Perform the retraction mapping  $\varphi_{\mathbf{Q}_c}^{-1}(\overline{\varphi_{\mathbf{Q}_c}(\mathbf{Q}_{[i]})})$  to obtain  $\mathbf{Q}_+$  defined in (3.10)
  - 5:   Assign  $\mathbf{Q}_c \leftarrow \mathbf{Q}_+$
  - 6: **end while**
  - 7: Output  $\overline{\mathbf{Q}} = \mathbf{Q}_c$
- 

More details of the algorithm are given below. For the choice of the initial iterate  $\mathbf{Q}_{\text{ini}}$ , we select the iterate that has the largest value of  $\text{tr}(\tilde{\Sigma}_{[i]})$  from the collection  $\{\mathbf{Q}_{[i]}\}_{i=1}^N$ , where  $\tilde{\Sigma}_{[i]}$  is the diagonal matrix consisting of the singular values of  $\mathbf{Y}_{[i]}$  computed in Step 2 of Algorithm 2. Specifically, we choose  $\mathbf{Q}_{\text{ini}} = \mathbf{Q}_{[i_{\text{max}}]}$ , where  $i_{\text{max}} = \text{argmax}_{i=1, \dots, N} \text{tr}(\tilde{\Sigma}_{[i]})$ . In each iteration, namely Steps 3 and 4 of Algorithm 3, we move the current iterate  $\mathbf{Q}_c$  to the next iterate  $\mathbf{Q}_+$  via the following procedure. One iteration of the integration Algorithm 3 is illustrated conceptually in Figure 3.1. In particular, Step 3 of Algorithm 3 is composed of the following two tasks.

1. As shown in Figure 3.1(a), we map (or lift) the matrices  $\{\mathbf{Q}_{[i]}\}_{i=1}^N$  to the tangent space  $\mathcal{T}_{\mathbf{Q}_c} \mathcal{S}_{m,\ell}$ . That is, each  $\mathbf{Q}_{[i]} \in \mathcal{S}_{m,\ell}$  is mapped to

$$\varphi_{\mathbf{Q}_c}(\mathbf{Q}_{[i]}) = (\mathbf{I}_m - \mathbf{Q}_c \mathbf{Q}_c^\top) \mathbf{Q}_{[i]} \mathbf{Q}_{[i]}^\top \mathbf{Q}_c \in \mathcal{T}_{\mathcal{S}_{m,\ell}, \mathbf{Q}_c}. \quad (3.8)$$

Because  $\mathbf{Q}_c^\top \{\varphi_{\mathbf{Q}_c}(\mathbf{Q}_{[i]})\} + \{\varphi_{\mathbf{Q}_c}(\mathbf{Q}_{[i]})\}^\top \mathbf{Q}_c = \mathbf{0}$ , we know that  $\varphi_{\mathbf{Q}_c}(\mathbf{Q}_{[i]})$  is indeed a point on  $\mathcal{T}_{\mathbf{Q}_c} \mathcal{S}_{m,\ell}$  [22].

2. As shown in Figure 3.1(b), we then take the average of the mapped matrix points. Because these mapped matrices are located on  $\mathcal{T}_{\mathbf{Q}_c} \mathcal{S}_{m,\ell}$ , which is a flat space, we can compute the arithmetic average of  $\varphi_{\mathbf{Q}_c}(\mathbf{Q}_{[i]})$

$$\overline{\varphi_{\mathbf{Q}_c}(\mathbf{Q}_{[i]})} = \frac{1}{N} \sum_{i=1}^N \varphi_{\mathbf{Q}_c}(\mathbf{Q}_{[i]}) = (\mathbf{I}_m - \mathbf{Q}_c \mathbf{Q}_c^\top) \overline{\mathbf{P}} \mathbf{Q}_c. \quad (3.9)$$

In (3.9), we apply (3.8) and the definition of  $\overline{\mathbf{P}}$  in (2.6). This average is still on the tangent space. Furthermore,  $\overline{\varphi_{\mathbf{Q}_c}(\mathbf{Q}_{[i]})} = \mathbf{D}_F(\mathbf{Q}_c)$  by (3.5).

In Step 4, as shown in Figure 3.1(c), we pull the averaged matrix  $\overline{\varphi_{\mathbf{Q}_c}(\mathbf{Q}_{[i]})}$  back to the Stiefel manifold by the inverse map  $\varphi_{\mathbf{Q}_c}^{-1}$ . Specifically,

$$\mathbf{Q}_+ = \varphi_{\mathbf{Q}_c}^{-1}(\overline{\varphi_{\mathbf{Q}_c}(\mathbf{Q}_{[i]})}) = \mathbf{Q}_c \mathbf{C} + \overline{\varphi_{\mathbf{Q}_c}(\mathbf{Q}_{[i]})} \mathbf{C}^{-1}, \quad (3.10)$$

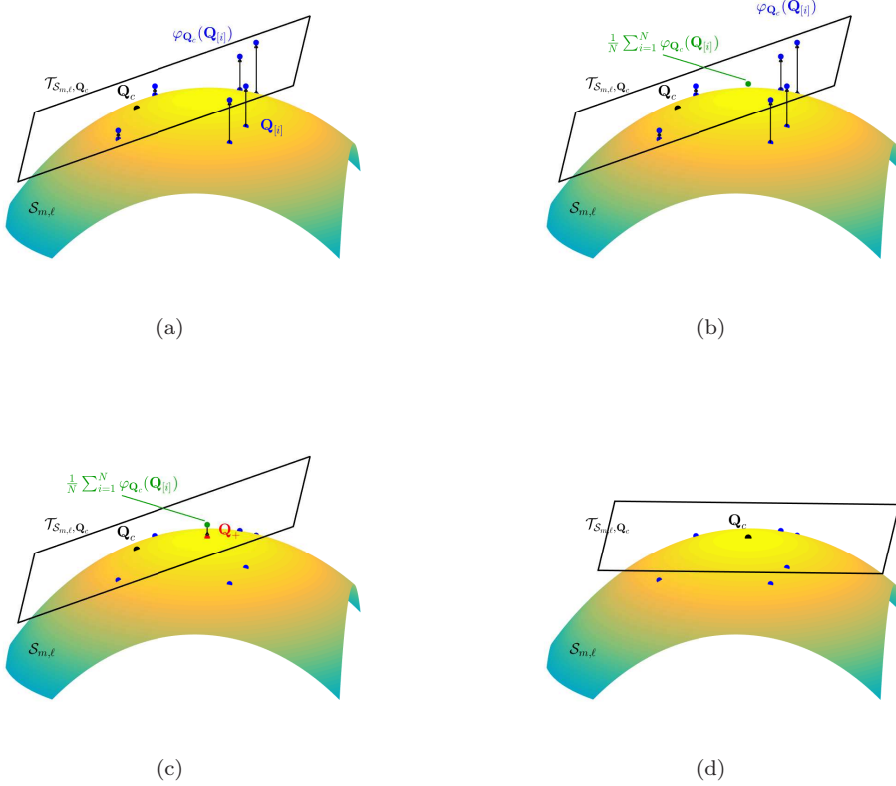


Fig. 3.1: A conceptual illustration of one iteration of Algorithm 3 for solving the optimization problem (2.7). (a) Five  $\mathbf{Q}_{[i]}$  (blue dots) on the Stiefel manifold  $\mathcal{S}_{m,\ell}$  are lifted to  $\varphi_{\mathbf{Q}_c}(\mathbf{Q}_{[i]}\mathbf{Q}_{[i]}^\top)$  on the tangent space  $\mathcal{T}_{\mathbf{Q}_c}\mathcal{S}_{m,\ell}$  corresponding to the current iterate  $\mathbf{Q}_c$  (black dot). (b) We compute the KN-type average of the lifted points, which is identified by the green point. (c) The average of the lifted points (green dot) is mapped back to the  $\mathbf{Q}_+$  (red dot) on the Stiefel manifold as the next iterate. (d) We have moved from  $\mathbf{Q}_c$  to  $\mathbf{Q}_+$  and obtained the new  $\mathbf{Q}_c$ .

where  $\mathbf{C} = \left[ \frac{\mathbf{I}_\ell}{2} + \left[ \frac{\mathbf{I}_\ell}{4} - \overline{\varphi_{\mathbf{Q}_c}(\mathbf{Q}_{[i]})}^\top \overline{\varphi_{\mathbf{Q}_c}(\mathbf{Q}_{[i]})} \right]^{1/2} \right]^{1/2}$  by Theorem 3.4 with fixed  $\tau = 1$ .

In short, we move the iterate from  $\mathbf{Q}_c$  to  $\mathbf{Q}_+$  in the loop of Algorithm 3 by the following procedure. (i)  $\mathbf{Q}_{[i]}$  are mapped to  $\mathcal{T}_{\mathbf{Q}_c}\mathcal{S}_{m,\ell}$  by  $\varphi_{\mathbf{Q}_c}$ , (ii) the mapped matrices are averaged as  $\overline{\varphi_{\mathbf{Q}_c}(\mathbf{Q}_{[i]})} = \mathbf{D}_F(\mathbf{Q}_c)$ , and finally, (iii)  $\mathbf{D}_F(\mathbf{Q}_c)$  is mapped back to the manifold by the inverse map  $\varphi_{\mathbf{Q}_c}^{-1}$  to obtain the next iterate  $\mathbf{Q}_+$ . This process can be summarized in one line:  $\mathbf{Q}_+ \leftarrow \varphi_{\mathbf{Q}_c}^{-1} \left( \frac{1}{N} \sum_{i=1}^N \varphi_{\mathbf{Q}_c}(\mathbf{Q}_{[i]}) \right)$ .

**3.5. Convergence and Remarks.** Algorithm 3 is a fixed-point iteration with step size  $\tau = 1$ . The update from the current  $\mathbf{Q}_c$  to the next  $\mathbf{Q}_+$  can be written as

$$\mathbf{Q}_+ = g(\mathbf{Q}_c) = \mathbf{Q}_c \mathbf{C} + \mathbf{X} \mathbf{C}^{-1}, \quad (3.11)$$

where  $\mathbf{C}$  and  $\mathbf{X}$  both depend on  $\mathbf{Q}_c$  and can be denoted as  $\mathbf{C}(\mathbf{Q}_c)$  and  $\mathbf{X}(\mathbf{Q}_c)$ , respectively. Recall that Algorithm 3 is used to find the maximizer of the objective function  $F(\mathbf{Q}) = \frac{1}{2} \text{tr}(\mathbf{Q}^\top \overline{\mathbf{P}} \mathbf{Q})$ . Let  $\mathbf{Q}_*$  consist of the leading  $\ell$  eigenvectors of  $\overline{\mathbf{P}}$ . Specifically,  $\mathbf{Q}_*$  consists of the maximizer (uniquely up to an orthogonal transformation) of the objective function  $F(\mathbf{Q})$ . Further, let  $\mathcal{N}_\varepsilon(\mathbf{Q}_*) := \{\mathbf{Q} \in \mathcal{S}_{m,\ell} : \|\mathbf{Q} - \mathbf{Q}_*\|_F < \varepsilon\}$  be an  $\varepsilon$ -neighborhood of  $\mathbf{Q}_*$  in  $\mathcal{S}_{m,\ell}$ . We can see that  $\mathbf{Q}_*$  is a fixed point for  $g$  in (3.11). We establish the convergence for the fixed-point iteration in Theorem 3.5. The theorem suggests that Algorithm 3 converges if it starts from an initial iterate that belongs to the  $\varepsilon$ -neighborhood of an equivalent version of  $\mathbf{Q}_*$ . The equivalence is in the sense of an orthogonal transformation multiplied on the right side of  $\mathbf{Q}_*$ . The proof of Theorem 3.5 is given in Appendix A.8.

**THEOREM 3.5.** *There exists an  $\varepsilon > 0$  such that Algorithm 3 converges, provided that the iteration starts from an initial  $\mathbf{Q}_{\text{ini}} \in \mathcal{N}_\varepsilon(\mathbf{Q}_* \mathbf{R}_0)$ , where  $\mathbf{R}_0$  is an arbitrary orthogonal matrix.*

We conclude the discussion of Algorithm 3 with the following remarks. First, we bridge the theoretical aspect of the optimal representation  $\overline{\mathbf{Q}}$  and the numerical scheme shown in Algorithm 3. Because  $\overline{\mathbf{Q}}$  is the solution of the optimization problem (2.7), we have  $\mathbf{D}_F(\overline{\mathbf{Q}}) = \mathbf{0}$ . Equation (3.5) further suggests that  $\frac{1}{N} \sum_{i=1}^N \varphi_{\overline{\mathbf{Q}}}(\mathbf{Q}_{[i]}) = \mathbf{0}$ . Moreover, by the definition (3.1), we can obtain the Kolmogorov-Nagumo-type average of  $\mathbf{Q}_{[i]}$  in terms of  $\overline{\mathbf{Q}}$ :

$$\varphi_{\overline{\mathbf{Q}}}^{-1} \left( \frac{1}{N} \sum_{i=1}^N \varphi_{\overline{\mathbf{Q}}}(\mathbf{Q}_{[i]}) \right) = \varphi_{\overline{\mathbf{Q}}}^{-1}(\mathbf{0}) = \overline{\mathbf{Q}}. \quad (3.12)$$

The last equality holds because of the following. For  $\mathbf{X} = \mathbf{0}$ , Equation (3.7) suggests that

$$\mathbf{C} = \mathbf{I}_\ell, \quad (3.13)$$

and Equation (3.6) further suggests that  $\varphi_{\overline{\mathbf{Q}}}^{-1}(\mathbf{0}) = \overline{\mathbf{Q}}$ . Equation (3.12) indicates that the optimal representation  $\overline{\mathbf{Q}}$  is a Kolmogorov-Nagumo type average and also a fixed point in Algorithm 3 with the corresponding projected gradient equal to zero. These facts represent a theoretical background for computing  $\overline{\mathbf{Q}}$ , and Algorithm 3 provides a numerical method to compute  $\overline{\mathbf{Q}}$ .

Second, we use small  $\|\mathbf{C} - \mathbf{I}_\ell\|$  as the stopping criterion on Step 2 of Algorithm 3 based on the fact shown in (3.13). This choice of stopping criterion can be viewed from the small change between  $\mathbf{Q}_+$  and  $\mathbf{Q}_c$ . When  $\mathbf{C}$  is close to the identity matrix,  $\mathbf{Q}_+$  is close to  $\mathbf{Q}_c$ . It is worth mentioning that  $\mathbf{C}$  is a small matrix with dimensions  $\ell \times \ell$  and is computed in the iteration of Algorithm 3. Therefore, the stopping criterion does not require extra computational effort.

Third, the constrained maximization problem (2.7) can be solved using the gradient ascent method proposed in [23]. The method starts from an initial  $\mathbf{Q}_{\text{ini}} \in \mathcal{S}_{m,\ell}$  and updates the current iterate  $\mathbf{Q}_c$  by searching the next iterate  $\mathbf{Q}_+$  on a curve lying on the Stiefel manifold  $\mathcal{S}_{m,\ell}$  to satisfy the orthogonality constraint. The curve is obtained by mapping the projected gradient defined in (3.3) to the Stiefel manifold

via a Cayley transform. An efficient step size selection along the curve can accelerate the overall convergence. On the other hand, Theorem 3.4 presents a curve along the direction of the projected gradient on the manifold. In Algorithm 3, it is equivalent to setting the step size as  $\tau = 1$ , and Algorithm 3 can consequently be viewed as a gradient ascent method.

We have proposed and analyzed Algorithm 3 to compute  $\overline{\mathbf{Q}}$  by solving the constrained optimization (2.7) (and (2.3) equivalently). With the computed  $\overline{\mathbf{Q}}$ , we can use iSVD, i.e., Algorithm 2, to perform the approximate SVD defined in (2.2) with multiple random sketches. In the next section, the iSVD is analyzed statistically.

**4. Statistical Analysis.** In this section, we present some theoretic statistical analysis on iSVD. First, we prove a Strong Law of Large Numbers (SLNN) result in Theorem 4.1 to show that iSVD (2.2) can perform as well as the full data SVD (1.1) as the number of random sketches  $N$  goes to infinity. Next, consistencies in terms of subspace and singular vectors are asserted in Theorem 4.3. Finally, we determine a rate of convergence by the Central Limit Theorem (CLT) in Theorem 4.4.

**Strong Law of Large Numbers.** From Theorem 2.1 and the fact that the absolute values of entries of a projection matrix are bounded by one, we have the following immediate result based on Theorem 2.1.

THEOREM 4.1 (Strong Law of Large Numbers). *We have*

$$\lim_{N \rightarrow \infty} \frac{1}{N} \sum_{i=1}^N \mathbf{Q}_{[i]} \mathbf{Q}_{[i]}^\top = \mathbf{U} \mathbf{\Lambda} \mathbf{U}^\top \quad \text{with probability one,}$$

where  $\mathbf{\Lambda}$  is given in Theorem 2.1 and  $\mathbf{U}$  is the true left singular vectors of the underlying matrix  $\mathbf{A}$  in decreasing order.

**Consistency.** Next, we establish the consistency between the left singular vectors computed by iSVD and the true left singular vectors. We prove Lemma 4.2 first. Based on the lemma, we prove the consistency in Theorem 4.3. See Appendix A.9 for the proofs of the lemma and the theorem.

LEMMA 4.2. *Let  $\mathbf{U} = [\mathbf{u}_1, \dots, \mathbf{u}_m]$  be an arbitrary point in  $\mathcal{S}_{m,m}$ , and let  $\mathbf{\Lambda}$  be a diagonal matrix with decreasing diagonal entries  $1 > \lambda_1 \geq \lambda_2 \geq \dots \lambda_\ell > \lambda_{\ell+1} \geq \dots \geq \lambda_m \geq 0$ . Consider the following minimization problem:*

$$\mathbf{Q}_{\text{opt}} = \underset{\mathbf{Q} \in \mathcal{S}_{m,\ell}}{\text{argmin}} \|\mathbf{U} \mathbf{\Lambda} \mathbf{U}^\top - \mathbf{Q} \mathbf{Q}^\top\|_F^2.$$

Then, we have  $\mathbf{Q}_{\text{opt}} \mathbf{Q}_{\text{opt}}^\top = \mathbf{U}_\ell \mathbf{U}_\ell^\top$ , where  $\mathbf{U}_\ell = [\mathbf{u}_1, \dots, \mathbf{u}_\ell]$ .

THEOREM 4.3 (Consistency of subspaces and singular vectors.). *Assume that the diagonal entries of  $\mathbf{\Sigma}$  (i.e., singular values of  $\mathbf{A}$ ) satisfy the condition:  $\sigma_1 > \sigma_2 > \dots > \sigma_\ell > \sigma_{\ell+1} \geq \dots \geq \sigma_m \geq 0$ . Then, we have the following properties. (a)  $\lim_{N \rightarrow \infty} \overline{\mathbf{Q}} \overline{\mathbf{Q}}^\top = \mathbf{U}_\ell \mathbf{U}_\ell^\top$  with probability one. (b) Let  $\widehat{\mathbf{W}}_\ell$  consist of the left singular vectors of  $\overline{\mathbf{Q}}^\top \mathbf{A}$ , and let  $\widehat{\mathbf{U}}_\ell = \overline{\mathbf{Q}} \widehat{\mathbf{W}}_\ell$  as described in Algorithm 2. Then, for any  $j \leq \ell$ , we have*

$$\lim_{N \rightarrow \infty} |\widehat{\mathbf{u}}_j^\top \mathbf{u}_j| = 1 \quad \text{with probability one,}$$

where  $\widehat{\mathbf{u}}_j$  is the  $j$ th column of  $\widehat{\mathbf{U}}_\ell$  and  $\mathbf{u}_j$  is the  $j$ th column of  $\mathbf{U}_\ell$ .

Note that the consistency established in Theorem 4.3 is valid for the entire  $\widehat{\mathbf{U}}_\ell$ , where  $\ell$  is the sampling dimension. However, we expect a more accurate  $\widehat{\mathbf{U}}_k$  using a larger sampling dimension  $\ell$ . See Table 1.1 for the definitions of  $k$  and  $\ell$ .

**Central Limit Theorems.** Because  $\mathbf{Q}_{[1]}, \mathbf{Q}_{[2]}, \dots, \mathbf{Q}_{[N]}$  are i.i.d., so are  $\mathbf{Q}_{[1]}\mathbf{Q}_{[1]}^\top, \mathbf{Q}_{[2]}\mathbf{Q}_{[2]}^\top, \dots, \mathbf{Q}_{[N]}\mathbf{Q}_{[N]}^\top$ ; and they have finite second moments. The following theorem is an immediate CLT result from Theorem 2.1.

THEOREM 4.4 (Central Limit Theorem I). *We have*

$$\frac{1}{\sqrt{N}} \sum_{i=1}^N \text{vec} \left( \mathbf{Q}_{[i]}\mathbf{Q}_{[i]}^\top - \mathbf{U}\mathbf{\Lambda}\mathbf{U}^\top \right) \overset{d}{\rightsquigarrow} \mathcal{N}(\mathbf{0}, \mathbf{T}_1), \quad \text{as } N \rightarrow \infty, \quad (4.1)$$

where  $\mathbf{T}_1$  is a certain positive definite matrix.

Theorem 4.4 is a CLT on the average of projection matrices. However, a more sensible CLT should be for the singular vectors  $\hat{\mathbf{u}}_j$  estimated by iSVD. Note that  $\hat{\mathbf{u}}_j$  (or  $\mathbf{u}_j$ ) is a function of  $\frac{1}{N} \sum_{i=1}^N \mathbf{Q}_{[i]}\mathbf{Q}_{[i]}^\top$  (or  $\mathbf{U}\mathbf{\Lambda}\mathbf{U}^\top$ ). By the delta-method to (4.1), we can establish the following CLT on  $\hat{\mathbf{u}}_j$ . See Appendix A.10 for the proof.

THEOREM 4.5 (Central Limit Theorem II). *We have*

$$\sqrt{N} (\hat{\mathbf{u}}_j - \mathbf{u}_j) \overset{d}{\rightsquigarrow} \mathcal{N}(\mathbf{0}, \mathbf{T}_2), \quad \text{as } N \rightarrow \infty,$$

where  $\mathbf{T}_2 = \mathbf{\Delta}_j \mathbf{T}_1 \mathbf{\Delta}_j^\top$  and  $\mathbf{\Delta}_j = \frac{\partial \mathbf{u}_j}{\partial \text{vec}(\mathbf{U}\mathbf{\Lambda}\mathbf{U}^\top)}$  is given by (A.14) below.

From Theorem 4.5, we know that  $\hat{\mathbf{u}}_j - \mathbf{u}_j = O_p(N^{-1/2})$  and so is  $\hat{\mathbf{U}}_\ell - \mathbf{U}_\ell = O_p(N^{-1/2})$ . Then,  $\|\hat{\mathbf{U}}_\ell \hat{\mathbf{U}}_\ell^\top - \mathbf{U}_\ell \mathbf{U}_\ell^\top\|_F^2 = O_p(N^{-1})$  and  $\|\hat{\mathbf{U}}_\ell \hat{\mathbf{U}}_\ell^\top - \mathbf{U}_\ell \mathbf{U}_\ell^\top\|_{\text{sp}} = O_p(N^{-1/2})$ . Note that  $\hat{\mathbf{U}}_\ell \hat{\mathbf{U}}_\ell^\top = \overline{\mathbf{Q}} \overline{\mathbf{Q}}^\top$ . From  $\|\mathbf{U}_\ell \mathbf{\Sigma}_\ell \mathbf{V}_\ell - \mathbf{A}\|_F^2 = \sigma_{k+1}^2 + \dots + \sigma_m^2$  and  $\|\mathbf{U}_\ell \mathbf{\Sigma}_\ell \mathbf{V}_\ell - \mathbf{A}\|_{\text{sp}} = \sigma_{k+1}$ , we have

$$\|\overline{\mathbf{Q}} \overline{\mathbf{Q}}^\top \mathbf{A} - \mathbf{A}\|_F^2 = \sigma_{k+1}^2 + \dots + \sigma_m^2 + O_p(N^{-1}) \quad (4.2)$$

and

$$\|\overline{\mathbf{Q}} \overline{\mathbf{Q}}^\top \mathbf{A} - \mathbf{A}\|_{\text{sp}}^2 = \sigma_{k+1}^2 + O_p(N^{-1}). \quad (4.3)$$

Specifically, as  $N \rightarrow \infty$ , we can achieve tight bounds in both the Frobenius norm and the spectral norm by integrating multiple random sketches.

**5. Numerical Results.** We conduct numerical experiments to study the performance of the proposed algorithms. To test the proposed iSVD, we construct the following test matrices, which are similar to the test matrices used in [17]. Let the matrix  $\mathbf{A} = \mathbf{H}_d \mathbf{\Sigma} \mathbf{H}_{d+1}^\top \in \mathbb{R}^{2^d \times 2^{d+1}}$ , where  $\mathbf{H}_d$  is the Hadamard matrix of size  $2^d \times 2^d$  and  $\mathbf{\Sigma}$  is a diagonal matrix of size  $2^d \times 2^{d+1}$ . Note that, for a Hadamard matrix,  $\mathbf{H}_d^\top = \mathbf{H}_d$  and  $\mathbf{H}_d^\top \mathbf{H}_d = \mathbf{I}_{2^d}$ . Let the desired rank be  $k = 10$ . We set the  $j$ th diagonal entry of  $\mathbf{\Sigma}$  as follows:

$$\Sigma_{j,j} = \sigma_j = \begin{cases} \sigma_1^{\lfloor j/2 \rfloor / 5}, & j = 1, 3, 5, 7, 9, \\ 1.5\sigma_{j+1} & j = 2, 4, 6, 8, 10, \\ 0.001, & j = 11, \\ \sigma_{11} \cdot \frac{m-j}{m-11}, & j = 12, \dots, m. \end{cases} \quad (5.1)$$

Here,  $\lfloor j/2 \rfloor$  is the greatest integer less than or equal to  $j/2$ . Our  $\mathbf{\Sigma}$  is modified from [17] to distinguish the singular values, and thus, individual singular vectors can be uniquely identified. Note that  $\mathbf{H}_d$  is an orthogonal matrix. Thus, the SVD of the

test matrix  $\mathbf{A}$  is known to be  $\mathbf{H}_d \boldsymbol{\Sigma} \mathbf{H}_{d+1}^\top$ , where the columns of  $\mathbf{H}_d$  and  $\mathbf{H}_{d+1}$  are the left and right singular vectors, respectively, and  $\sigma_j$  are singular values.

The experimental settings are  $d = 9, 11, 13, 15, 17, 19$ ,  $k = 10$ ,  $p = 12$ ,  $\ell = k + p = 22$ ,  $q = 0, 1$ , and  $N = 10, 50, 100, 200$ . For an initial  $\mathbf{Q}_{\text{ini}}$ , we select from the collection  $\{\mathbf{Q}_{[i]}\}_{i=1}^N$ . We choose the  $\mathbf{Q}_{[i]}$  that has the largest value of  $\text{tr}(\tilde{\boldsymbol{\Sigma}}_{[i]})$ , where  $\tilde{\boldsymbol{\Sigma}}_{[i]}$  is the diagonal matrix consisting of the singular values of  $\mathbf{Y}_{[i]}$  computed in Step 2 of Algorithm 2. To evaluate the accuracy of approximate SVD, we use the following similarity for comparing the computed and true leading  $k$  individual singular vectors. Recall that  $\tilde{\mathbf{U}}_k = \{\tilde{\mathbf{u}}_1, \dots, \tilde{\mathbf{u}}_j, \dots, \tilde{\mathbf{u}}_k\}$  and  $\hat{\mathbf{U}}_k = \{\hat{\mathbf{u}}_1, \dots, \hat{\mathbf{u}}_j, \dots, \hat{\mathbf{u}}_k\}$  consist of the rank- $k$  left singular vectors computed by Algorithm 1 (rSVD) and Algorithm 2 (iSVD), respectively.  $\mathbf{U}_k = \{\mathbf{u}_1, \dots, \mathbf{u}_j, \dots, \mathbf{u}_k\}$  consists of the true left singular vectors of  $\mathbf{A}$ . We measure the similarity between the  $j$ th computed singular vector  $\tilde{\mathbf{u}}_j$  (or  $\hat{\mathbf{u}}_j$ ) and the true singular vector  $\mathbf{u}_j$  by computing  $|\tilde{\mathbf{u}}_j^\top \mathbf{u}_j|$  (or  $|\hat{\mathbf{u}}_j^\top \mathbf{u}_j|$ ) for  $j = 1, \dots, k$ . If the computed singular vector has no error, then  $|\tilde{\mathbf{u}}_j^\top \mathbf{u}_j| = 1$  (or  $|\hat{\mathbf{u}}_j^\top \mathbf{u}_j| = 1$ ). Note that we present only the results regarding the left singular vectors. The results involving the right singular vectors are similar and ignored here. Algorithm 3 is stopped if  $\|\mathbf{C} - \mathbf{I}_\ell\|_F$  is less than  $10^{-5}$ . The numerical experiments are conducted on a workstation equipped with an Intel E5-2650 v3 CPU (with a 25 MB cache and 2.30 GHz clock rate) and 256 GB of main memory. The algorithms are implemented in MATLAB version 2015b.

We report the accuracies and variations in the computed singular values and singular vectors in Figure 5.1 and Table 5.1 using different parameters. We highlight the following observations.

- *The similarity (accuracy) of the singular vectors increases as the number of random sketches  $N$  increases.* For each singular vector, we examine the accuracy performance in terms of the similarity between the computed and true singular vector. Figure 5.1 shows the singular vector similarity results with box plots. In the figure, the matrix size is  $2^{19} \times 2^{20}$  ( $d = 19$ ), the sampling dimension  $\ell = 22$ , the number of random sketches  $N = 1, 10, 50, 100$ , and 200, and the exponent of the power method in Step 2 of Algorithms 1 and 2 (i.e.,  $q$ ) equals 0 or 1. Higher similarities (up to 1) are better. It is clear that larger  $N$  results in higher similarity in all the tested cases. Some of the improvements can be significant, especially for several cases when  $q = 0$  and the 9th singular vector for  $q = 1$ . Note that the 10th singular vector is difficult to compute. This is because the 10th eigenvalue belongs to a cluster of singular values, and it is difficult to distinguish the singular vectors of these slow-decaying singular values.
- *The rank- $k$  matrix error decreases as the number of random sketches  $N$  increases.* We also examine the accuracy performance with respect to the combination of the singular values and singular vectors. In particular, we compute the rank- $k$  matrix error  $\|\mathbf{U}_k \boldsymbol{\Sigma}_k \mathbf{V}_k^\top - \hat{\mathbf{U}}_k \hat{\boldsymbol{\Sigma}}_k \hat{\mathbf{V}}_k^\top\|_F$ . This error evaluates the difference between the estimated and true rank- $k$  SVD. We experiment with different  $d$  to better present the trend of the integration effect for  $d$ . The observations hold for all the experiments for  $d = 9, 11, 13, 15, 17$ , and 19 with  $q = 0$  and  $q = 1$ , as shown in Table 5.1.
- *Overall, the stochastic variation in similarity of a singular vector to its target decreases as the number of random sketches  $N$  increases.* This welcomed result can be expected because more random sketches have been integrated, and thus, the averaged sketch becomes more stable and with less stochastic



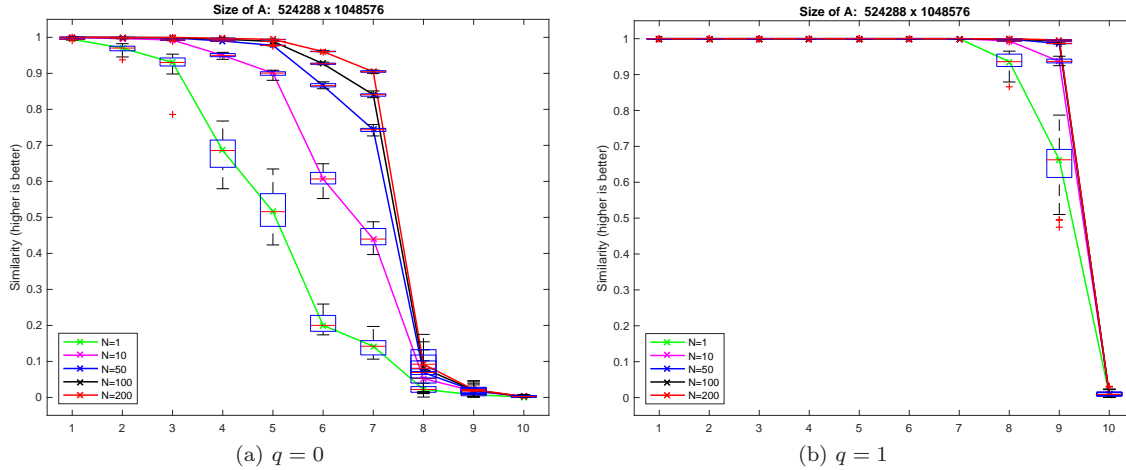


Fig. 5.1: The similarity results for  $d = 19$ ,  $\ell = 22$ ,  $q = 0, 1$ , and  $N = 1, 10, 50, 100, 200$ . The figure also shows the box plots indicating the median and the 25th and 75th percentiles of the similarities out of 30 replicated runs. Higher similarities (up to 1) are better.

variation. Such an observation holds for almost all the numerical results shown in Table 5.1.

Furthermore, we investigate the effect of increasing the sampling dimension  $\ell$  for rSVD ( $N = 1$ ) and compare the results with iSVD ( $N > 1$ ), which uses  $\ell = 22$  and  $N = 200$ , resulting in  $\ell \times N = 4400$  samples in total. In these numerical experiments,  $d = 19$ ,  $q = 0$ , and the number of replicated runs is 30. Table 5.2 shows the Frobenius norm of the error matrix (i.e.,  $\|\mathbf{U}_k \Sigma_k \mathbf{V}_k^\top - \tilde{\mathbf{U}}_k \tilde{\Sigma}_k \tilde{\mathbf{V}}_k^\top\|_F$  for rSVD and  $\|\mathbf{U}_k \Sigma_k \mathbf{V}_k^\top - \hat{\mathbf{U}}_k \hat{\Sigma}_k \hat{\mathbf{V}}_k^\top\|_F$  for iSVD). Two main observations are highlighted below.

- *In rSVD ( $N = 1$ ), a larger  $\ell$  results in smaller average errors and smaller standard deviations.* This observation is reasonable because when we sketch a greater number of sampling dimensions, more information of the leading singular vectors is collected.
- *SVD computed by iSVD with smaller sampling dimensions (via multiple sketches) is better than rSVD with large sampling dimensions (via a single sketch).* We compare the result obtained by iSVD with  $\ell = 22$  and  $N = 200$  (4400 sampling dimensions in total) with the results obtained by rSVD with various  $\ell$  and  $N = 1$ . As shown in Table 5.2, iSVD outperforms rSVD in all cases except for the case with  $\ell = 4400$ . For the case in which  $\ell = 4400$ , rSVD performs slightly better. This observation suggests the advantage of integration. In addition, even without adopting parallelism, taking 200 random sketches with  $\ell = 22$  and integrating them is relatively efficient compared to executing an rSVD with  $\ell = 3000$  in terms of both precision and time.

**6. Conclusions.** We have proposed and analyzed a Monte Carlo-type algorithm for computing the rank- $k$  SVD of large matrices. The proposed algorithm integrates multiple leading low-dimensional subspaces projected by multiple random sketches.

d	N=1	N=10	N=50	N=100	N=200
(a) $q = 0$					
9	1.04e-02 (6.56e-04)	3.79e-03 (1.18e-04)	1.74e-03 (4.37e-05)	1.23e-03 (2.46e-05)	8.71e-04 (1.52e-05)
11	1.89e-02 (1.12e-03)	6.74e-03 (1.51e-04)	3.25e-03 (5.94e-05)	2.32e-03 (3.07e-05)	1.67e-03 (1.90e-05)
13	3.49e-02 (2.69e-03)	1.22e-02 (2.44e-04)	5.83e-03 (5.45e-05)	4.32e-03 (2.69e-05)	3.30e-03 (1.63e-05)
15	6.20e-02 (4.20e-03)	2.21e-02 (4.15e-04)	1.06e-02 (9.62e-05)	7.78e-03 (3.94e-05)	5.72e-03 (2.11e-05)
17	1.12e-01 (5.76e-03)	4.03e-02 (8.24e-04)	1.95e-02 (1.72e-04)	1.44e-02 (7.94e-05)	1.09e-02 (5.12e-05)
19	1.92e-01 (1.26e-02)	7.14e-02 (1.59e-03)	3.52e-02 (2.93e-04)	2.60e-02 (1.61e-04)	1.95e-02 (6.30e-05)
(b) $q = 1$					
9	1.08e-03 (1.50e-04)	4.30e-04 (3.55e-05)	1.95e-04 (1.40e-05)	1.37e-04 (8.63e-06)	9.75e-05 (5.96e-06)
11	1.53e-03 (1.03e-04)	7.61e-04 (3.89e-05)	3.68e-04 (1.43e-05)	2.62e-04 (1.06e-05)	1.87e-04 (6.84e-06)
13	1.83e-03 (5.54e-05)	1.23e-03 (4.43e-05)	6.89e-04 (2.00e-05)	5.05e-04 (1.32e-05)	3.65e-04 (7.55e-06)
15	2.14e-03 (9.61e-05)	1.64e-03 (4.45e-05)	1.17e-03 (2.59e-05)	9.27e-04 (1.61e-05)	7.22e-04 (1.26e-05)
17	2.97e-03 (2.81e-04)	1.93e-03 (2.30e-05)	1.78e-03 (7.72e-06)	1.75e-03 (8.45e-06)	1.74e-03 (9.44e-06)
19	4.14e-03 (2.77e-04)	2.35e-03 (5.20e-05)	1.89e-03 (6.91e-06)	1.82e-03 (2.81e-06)	1.78e-03 (9.79e-07)

Table 5.1: The average norm and standard deviation (in parentheses) of the error matrices (i.e.,  $\|\mathbf{U}\mathbf{\Sigma}\mathbf{V}^\top - \hat{\mathbf{U}}_k \hat{\mathbf{\Sigma}}_k \hat{\mathbf{V}}_k^\top\|_F$ ) over 30 replicated runs with various matrices of size  $2^d \times 2^{d+1}$ . The sampling dimension  $\ell = 22$  and the exponent  $q = 0$  or  $q = 1$ .

$\ell$	$N$ (Alg.)	Ave (std) of errors	$\ell$	$N$ (Alg.)	Ave (std) of errors
22	1 (rSVD)	1.90e-01 (1.39e-02)	3000	1 (rSVD)	2.06e-02 (9.16e-05)
500	1 (rSVD)	4.63e-02 (6.27e-04)	4400	1 (rSVD)	1.73e-02 (6.27e-05)
1000	1 (rSVD)	3.40e-02 (2.84e-04)	22	200 (iSVD)	1.95e-02 (6.30e-05)

Table 5.2: We use rSVD (with various sampling dimensions  $\ell$  and  $N = 1$ ) and iSVD (with  $\ell = 22$  and  $N = 200$ ) to compute the first 10 singular values and singular vectors. The table shows the averages (and standard deviations) of the error matrix norms (i.e.,  $\|\mathbf{U}\mathbf{\Sigma}\mathbf{V}^\top - \hat{\mathbf{U}}_k \hat{\mathbf{\Sigma}}_k \hat{\mathbf{V}}_k^\top\|_F$  for rSVD and  $\|\mathbf{U}\mathbf{\Sigma}\mathbf{V}^\top - \hat{\mathbf{U}}_k \hat{\mathbf{\Sigma}}_k \hat{\mathbf{V}}_k^\top\|_F$  for iSVD) out of 30 replicated runs. The matrix size is  $2^{19} \times 2^{20}$ , and the power exponent  $q = 0$ .

The integrated subspace is the solution of the optimization problem constrained by the matrix Stiefel manifold that best represents the multiple random projected subspaces. To solve the optimization problem, we propose an iterative method based on the Kolmogorov-Nagumo-type average of the multiple subspaces. Theoretical analyses reveal the insights of the proposed algorithms. Numerical experiments suggest that the integrated SVD can achieve higher accuracy and less stochastic variation in singular vectors using multiple random sketches.

It is interesting to generalize iSVD to other problems. First, we plan to investigate how iSVD performs if we replace the Gaussian random projections by the column random sampling. Unlike the Gaussian random projections, which involve matrix-matrix multiplications  $\mathbf{A}^\top \mathbf{A} \mathbf{\Omega}$ , the random column sampling can be implemented by column extractions without involving matrix-matrix multiplications, and therefore leads to a significant savings in computational time and memory usage, especially for large-scale matrices. However, the sketched subspaces contain less information about the leading subspaces, which may decrease the accuracy, and some statistical properties are different from the cases in Gaussian random projection. Other possible extensions of iSVD include eigenvalue problems, linear system problems, selected singular values within a given interval or of a given order, and tensor decompositions. Another future direction is to explore how we can efficiently compute the SVD if some of the columns or rows of  $\mathbf{A}$  are added (updated) or removed (downdated) after an

SVD has been obtained for a given matrix  $\mathbf{A}$ .

iSVD can be accelerated using multi-level parallelism. It is obvious the  $N$  random sketches can be performed simultaneously in parallel. The operations in each sketch and the integration process can be parallelized as well. Efficient implementations of the proposed algorithms on parallel computers will allow us to quickly estimate the SVD of large-scale matrices on GPUs, parallel computers, or distributed systems such as Spark [12].

In addition to the development of new algorithms and parallel implementations, the tuning of parameters can affect the timing and accuracy. Depending on the requirements (e.g., accuracy and number of singular values), matrix structures (e.g., sparsity, size, and distribution of the singular values), and computer architectures (e.g., multi-core CPU or GPU cluster), we can choose between  $N = 1$  (rSVD) and  $N > 1$  (iSVD), the power exponent  $q$ , and the oversampling size  $p$  (and thus the dimension of the random sketches  $\ell$ ). Fine-tuning of Algorithm 3 or gradient-based optimization methods may further improve the performance of iSVD. One example is the step size used to move from the current iterate to the next iterate.

In short, we have proposed and justified a new randomized algorithm to compute the approximate rank- $k$  SVD of a large matrix by integrating multiple leading subspaces based on random sketches. The framework can be further improved and extended to benefit data analytics, computational sciences and engineering in a broad manner.

**Acknowledgments.** This work is partially supported by the Ministry of Science and Technology, the National Center for Theoretical Sciences, and the Taida Institute for Mathematical Sciences in Taiwan.

#### REFERENCES

- [1] Haim Avron, Costas Bekas, Christos Boutsidis, Kenneth Clarkson, Prabhanjan Kambadur, Giorgos Kollias, Michael Mahoney, Yves Ineichen Ilse Ipsen, Vikas Sindhwani, and David Woodruff. libSkylark: an open source software library for distributed randomized numerical linear algebra with applications to machine learning and statistical data analysis. IBM Research, in collaboration with Bloomberg Labs, NCSU, Stanford, UC Berkeley, and Yahoo Labs. Available at <https://github.com/xdata-skylark/libskylark>., 2015.
- [2] Edouard Coakley, Vladimir Rokhlin, and Mark Tygert. A fast randomized algorithm for orthogonal projection. *SIAM Journal on Scientific Computing*, 33(2):849–868, 2011.
- [3] Laurent Demanet, Pierre-David Létourneau, Nicolas Boumal, Henri Calandra, Jiawei Chiu, and Stanley Snelson. Matrix probing: a randomized preconditioner for the wave-equation hessian. *Applied and Computational Harmonic Analysis*, 32(2):155–168, 2012.
- [4] Petros Drineas and Michael W. Mahoney. RandNLA: Randomized numerical linear algebra. *Commun. ACM*, 59(6):80–90, May 2016.
- [5] Simone Fiori, Tetsuya Kaneko, and Toshihisa Tanaka. Mixed maps for learning a kolmogoroff-nagumo-type average element on the compact Stiefel manifold. *IEEE International Conference on Acoustic, Speech and Signal Processing (ICASSP)*, pages 4518–4522, 2014.
- [6] Laura Grigori, Frédéric Nataf, Soleiman Yousef, et al. Robust algebraic schur complement preconditioners based on low rank corrections. 2014.
- [7] Ming Gu. Subspace iteration randomization and singular value problems. *SIAM Journal on Scientific Computing*, 37(3):A1139–A1173, 2015.
- [8] Nathan Halko, Per-Gunnar Martinsson, Yoel Shkolnisky, and Mark Tygert. An algorithm for the principal component analysis of large data sets. *SIAM Journal on Scientific computing*, 33(5):2580–2594, 2011.
- [9] Nathan Halko, Per-Gunnar Martinsson, and Joel A Tropp. Finding structure with randomness: Probabilistic algorithms for constructing approximate matrix decompositions. *SIAM review*, 53(2):217–288, 2011.
- [10] Nathan P Halko. Randomized methods for computing low-rank approximations of matrices. PhD thesis, University of Colorado, 2012.

- [11] Tetsuya Kaneko, Simone Fiori, and Toshihisa Tanaka. Empirical arithmetic averaging over the compact Stiefel manifold. IEEE Transactions on Signal Processing, 61(4):883–894, 2013.
- [12] Min Li, Jian Tan, Yandong Wang, Li Zhang, and Valentina Salapura. Sparkbench: a comprehensive benchmarking suite for in memory data analytic platform spark. In Proceedings of the 12th ACM International Conference on Computing Frontiers, page 53. ACM, 2015.
- [13] Jan R Magnus and Heinz Neudecker. The commutation matrix: some properties and applications. The Annals of Statistics, pages 381–394, 1979.
- [14] Michael W Mahoney. Randomized algorithms for matrices and data. Foundations and Trends in Machine Learning, 3(2):123–224, 2011.
- [15] Gunnar Martinsson. Randomized algorithms for very large-scale linear algebra.
- [16] Haifeng Qian and Sachin S Sapatnekar. Stochastic preconditioning for diagonally dominant matrices. SIAM Journal on Scientific Computing, 30(3):1178–1204, 2008.
- [17] Vladimir Rokhlin, Arthur Szlam, and Mark Tygert. A randomized algorithm for principal component analysis. SIAM Journal on Matrix Analysis and Applications, 31(3):1100–1124, 2009.
- [18] Vladimir Rokhlin and Mark Tygert. A fast randomized algorithm for overdetermined linear least-squares regression. Proceedings of the National Academy of Sciences, 105(36):13212–13217, 2008.
- [19] KK Sabelfeld. Stochastic boundary methods of fundamental solutions for solving pdes. Engineering Analysis with Boundary Elements, 36(7):1092–1103, 2012.
- [20] Thomas Strohmer and Roman Vershynin. A randomized solver for linear systems with exponential convergence. In Approximation, Randomization, and Combinatorial Optimization. Algorithms and Techniques, pages 499–507. Springer, 2006.
- [21] Arthur Szlam, Yuval Kluger, and Mark Tygert. An implementation of a randomized algorithm for principal component analysis. arXiv preprint arXiv:1412.3510, 2014.
- [22] Hemant D Tagare. Notes on optimization on stiefel manifolds. Technical report, Tech. Rep., Yale University, 2011.
- [23] Zaiwen Wen and Wotao Yin. A feasible method for optimization with orthogonality constraints. Mathematical Programming, 142(1-2):397–434, 2013.
- [24] Rafi Witten and Emmanuel Candès. Randomized algorithms for low-rank matrix factorizations: sharp performance bounds. Algorithmica, 72(1):264–281, 2013.
- [25] David P Woodruff. Sketching as a tool for numerical linear algebra. arXiv preprint arXiv:1411.4357, 2014.
- [26] Jianlin Xia, Yuanzhe Xi, and Ming Gu. A superfast structured solver for toeplitz linear systems via randomized sampling. SIAM Journal on Matrix Analysis and Applications, 33(3):837–858, 2012.
- [27] Hua Xiang and Jun Zou. Regularization with randomized svd for large-scale discrete inverse problems. Inverse Problems, 29(8):085008, 2013.
- [28] Ichitaro Yamazaki, Jakub Kurzak, Piotr Luszczek, and Jack Dongarra. Randomized algorithms to update partial singular value decomposition on a hybrid cpu/gpu cluster. In Proceedings of the International Conference for High Performance Computing, Networking, Storage and Analysis, page 59. ACM, 2015.
- [29] Jiyan Yang, Xiangrui Meng, and Michael W Mahoney. Implementing randomized matrix algorithms in parallel and distributed environments. Proceedings of the IEEE, 104(1):58–92, 2016.
- [30] Zhihua Zhang. The singular value decomposition, applications and beyond. arXiv preprint arXiv:1510.08532, 2015.

## Appendix.

**A.1. Proof of Theorem 2.1.** *Proof.* Since  $\Omega_{[i]}$  is a Gaussian random matrix, we have the expectation

$$\begin{aligned}
 E\left(\mathbf{Q}_{[i]}\mathbf{Q}_{[i]}^\top\right) &= E\left(\mathbf{A}\Omega_{[i]}\left(\Omega_{[i]}^\top\mathbf{A}^\top\mathbf{A}\Omega_{[i]}\right)^{-1}\Omega_{[i]}^\top\mathbf{A}^\top\right) \\
 &= \mathbf{U} E\left(\Sigma\mathbf{V}^\top\Omega_{[i]}\left(\Omega_{[i]}^\top\mathbf{V}\Sigma^2\mathbf{V}^\top\Omega_{[i]}\right)^{-1}\Omega_{[i]}^\top\mathbf{V}\Sigma\right) \mathbf{U}^\top =: \mathbf{U}\Lambda\mathbf{U}^\top,
 \end{aligned}$$

where

$$\Lambda = E\left(\Sigma\mathbf{V}^\top\Omega_{[i]}\left(\Omega_{[i]}^\top\mathbf{V}\Sigma^2\mathbf{V}^\top\Omega_{[i]}\right)^{-1}\Omega_{[i]}^\top\mathbf{V}\Sigma\right). \quad (\text{A.1})$$

Note that  $\mathbf{\Omega}_{[i]}^\top \mathbf{V} \mathbf{\Sigma}^2 \mathbf{V}^\top \mathbf{\Omega}_{[i]}$  is non-singular with probability one.

(a) *First, we show that  $\mathbf{\Lambda}$  is a diagonal matrix.* Its  $(j, j')$ th entry is given by

$$E \left( \sigma_j \sigma_{j'} \mathbf{z}_j^\top \left( \sum_{l=1}^m \sigma_l^2 \mathbf{z}_l \mathbf{z}_l^\top \right)^{-1} \mathbf{z}_{j'} \right),$$

where  $[\mathbf{z}_1, \dots, \mathbf{z}_n] = \mathbf{\Omega}_{[i]}^\top \mathbf{V}$ . Note that  $\mathbf{z}_j = \mathbf{\Omega}_{[i]}^\top \mathbf{v}_j$ , where  $\mathbf{v}_j$  is the  $j$ th column of  $\mathbf{V}$ . Let  $\boldsymbol{\omega}_l$  denote the  $l$ th column of  $\mathbf{\Omega}_{[i]}$ . Below we show that all off-diagonal entries of  $\mathbf{\Lambda}$  are zero. Without loss of generality, consider the  $(1, j)$ th entry of  $\mathbf{\Lambda}$ . Let  $\mathbf{V}_{-1} := [-\mathbf{v}_1, \mathbf{v}_2, \dots, \mathbf{v}_n]$  and  $\tilde{\mathbf{\Omega}}_{[i]} := \mathbf{V} \mathbf{V}_{-1}^\top \mathbf{\Omega}_{[i]}$ . Then,  $\tilde{\mathbf{\Omega}}_{[i]}^\top \mathbf{V} = \mathbf{\Omega}_{[i]}^\top \mathbf{V}_{-1} \mathbf{V}^\top \mathbf{V} = \mathbf{\Omega}_{[i]}^\top \mathbf{V}_{-1}$ . Let  $[\tilde{\mathbf{z}}_1, \dots, \tilde{\mathbf{z}}_n] := \tilde{\mathbf{\Omega}}_{[i]}^\top \mathbf{V}$ . Then,  $\tilde{\mathbf{z}}_1 = \tilde{\mathbf{\Omega}}_{[i]}^\top \mathbf{v}_1 = -\mathbf{z}_1$  and  $\tilde{\mathbf{z}}_j = \tilde{\mathbf{\Omega}}_{[i]}^\top \mathbf{v}_j = \mathbf{z}_j, \forall j \neq 1$ . Note that  $\mathbf{\Omega}_{[i]}$  and  $\tilde{\mathbf{\Omega}}_{[i]}$  have the same distribution, as  $\mathbf{\Omega}_{[i]}$  have i.i.d. Gaussian entries and  $(\mathbf{V} \mathbf{V}_{-1}^\top)^\top \mathbf{V} \mathbf{V}_{-1}^\top = \mathbf{I}$ . It implies that  $[\tilde{\mathbf{z}}_1, \dots, \tilde{\mathbf{z}}_n]$  and  $[\mathbf{z}_1, \dots, \mathbf{z}_n]$  follow the same distribution. That is,

$$\mathbf{z}_1^\top \left( \sum_{l=1}^m \sigma_l^2 \mathbf{z}_l \mathbf{z}_l^\top \right)^{-1} \mathbf{z}_j \stackrel{d}{=} \tilde{\mathbf{z}}_1^\top \left( \sum_{l=1}^m \sigma_l^2 \tilde{\mathbf{z}}_l \tilde{\mathbf{z}}_l^\top \right)^{-1} \tilde{\mathbf{z}}_j = -\mathbf{z}_1^\top \left( \sum_{l=1}^m \sigma_l^2 \mathbf{z}_l \mathbf{z}_l^\top \right)^{-1} \mathbf{z}_j,$$

where  $\stackrel{d}{=}$  means equal in distribution. Therefore, for the  $(1, j)$ th entry of  $\mathbf{\Lambda}$ , we have

$$E \left\{ \mathbf{z}_1^\top \left( \sum_{l=1}^m \sigma_l^2 \mathbf{z}_l \mathbf{z}_l^\top \right)^{-1} \mathbf{z}_j \right\} = -E \left\{ \mathbf{z}_1^\top \left( \sum_{l=1}^m \sigma_l^2 \mathbf{z}_l \mathbf{z}_l^\top \right)^{-1} \mathbf{z}_j \right\} = 0.$$

(b) *Next, we show that all the diagonals,  $E \left( \sigma_j^2 \mathbf{z}_j^\top \left( \sum_{l=1}^m \sigma_l^2 \mathbf{z}_l \mathbf{z}_l^\top \right)^{-1} \mathbf{z}_j \right)$ ,  $j = 1, \dots, n$ , are less than one.* Let  $\mathbf{B}_{(-j)} := \sum_{l \neq j}^m \sigma_l^2 \mathbf{z}_l \mathbf{z}_l^\top$ . As  $\mathbf{\Omega}_{[i]}$  consists of i.i.d. Gaussian entries and  $\ell < m$ ,  $\mathbf{B}_{(-j)}$  is strictly positive definite with probability one. By Sherman-Morrison-Woodbury matrix identity, we have

$$\left( \sum_{l=1}^m \sigma_l^2 \mathbf{z}_l \mathbf{z}_l^\top \right)^{-1} = \mathbf{B}_{(-j)}^{-1} - \frac{\sigma_j^2 \mathbf{B}_{(-j)}^{-1} \mathbf{z}_j \mathbf{z}_j^\top \mathbf{B}_{(-j)}^{-1}}{1 + \sigma_j^2 \mathbf{z}_j^\top \mathbf{B}_{(-j)}^{-1} \mathbf{z}_j}.$$

Then,

$$\begin{aligned} \sigma_j^2 \mathbf{z}_j^\top \left( \sum_{l=1}^m \sigma_l^2 \mathbf{z}_l \mathbf{z}_l^\top \right)^{-1} \mathbf{z}_j &= \sigma_j^2 \mathbf{z}_j^\top \left( \mathbf{B}_{(-j)}^{-1} - \frac{\sigma_j^2 \mathbf{B}_{(-j)}^{-1} \mathbf{z}_j \mathbf{z}_j^\top \mathbf{B}_{(-j)}^{-1}}{1 + \sigma_j^2 \mathbf{z}_j^\top \mathbf{B}_{(-j)}^{-1} \mathbf{z}_j} \right) \mathbf{z}_j \\ &= \sigma_j^2 \left( \mathbf{z}_j^\top \mathbf{B}_{(-j)}^{-1} \mathbf{z}_j - \frac{\sigma_j^2 \mathbf{z}_j^\top \mathbf{B}_{(-j)}^{-1} \mathbf{z}_j \mathbf{z}_j^\top \mathbf{B}_{(-j)}^{-1} \mathbf{z}_j}{1 + \sigma_j^2 \mathbf{z}_j^\top \mathbf{B}_{(-j)}^{-1} \mathbf{z}_j} \right) \\ &= \frac{\sigma_j^2 \mathbf{z}_j^\top \mathbf{B}_{(-j)}^{-1} \mathbf{z}_j}{1 + \sigma_j^2 \mathbf{z}_j^\top \mathbf{B}_{(-j)}^{-1} \mathbf{z}_j} = 1 - \frac{1}{1 + \sigma_j^2 \mathbf{z}_j^\top \mathbf{B}_{(-j)}^{-1} \mathbf{z}_j} < 1. \end{aligned} \tag{A.2}$$

(b) can be obtained by taking expectation of the inequality above.

(c) *Finally, we want to show that  $E \left\{ \sigma_j^2 \mathbf{z}_j^\top \left( \sum_{l=1}^m \sigma_l^2 \mathbf{z}_l \mathbf{z}_l^\top \right)^{-1} \mathbf{z}_j \right\}$  is strictly decreasing as  $j$  increases.* Without loss of generality, we will only show the comparison for  $j = 1, 2$ , i.e.,  $E \left\{ \sigma_1^2 \mathbf{z}_1^\top \left( \sum_{l=1}^m \sigma_l^2 \mathbf{z}_l \mathbf{z}_l^\top \right)^{-1} \mathbf{z}_1 \right\} > E \left\{ \sigma_2^2 \mathbf{z}_2^\top \left( \sum_{l=1}^m \sigma_l^2 \mathbf{z}_l \mathbf{z}_l^\top \right)^{-1} \mathbf{z}_2 \right\}$ .

Consider  $\tilde{\boldsymbol{\Omega}}_{[i]} := \mathbf{V}\mathbf{V}_{1,2}^\top \boldsymbol{\Omega}_{[i]}$ , where  $\mathbf{V}_{1,2} := [\mathbf{v}_2, \mathbf{v}_1, \mathbf{v}_3, \dots, \mathbf{v}_n]$ . Let  $[\mathbf{x}_1, \mathbf{x}_2, \dots, \mathbf{x}_n] := \tilde{\boldsymbol{\Omega}}_{[i]}^\top \mathbf{V}$ . Then,  $\mathbf{x}_1 = \mathbf{z}_2$ ,  $\mathbf{x}_2 = \mathbf{z}_1$ , and  $\mathbf{x}_j = \mathbf{z}_j$  for all  $3 \leq j \leq n$ . Similar to (A.2),

$$\sigma_j^2 \mathbf{x}_j^\top \left( \sum_{l=1}^m \sigma_l^2 \mathbf{x}_l \mathbf{x}_l^\top \right)^{-1} \mathbf{x}_j = 1 - \frac{1}{1 + \sigma_j^2 \mathbf{x}_j^\top \tilde{\mathbf{B}}_{(-j)}^{-1} \mathbf{x}_j}, \quad (\text{A.3})$$

where  $\tilde{\mathbf{B}}_{(-j)} := \sum_{l \neq j}^m \sigma_l^2 \mathbf{x}_l \mathbf{x}_l^\top$ . Again, we only need to consider the case that  $\tilde{\mathbf{B}}_{(-j)}$  is of full rank, which holds with probability one. Observe that  $\tilde{\mathbf{B}}_{(-2)} = \mathbf{B}_{(-1)} + (\sigma_1^2 - \sigma_2^2) \mathbf{z}_2 \mathbf{z}_2^\top$ . Then,

$$\begin{aligned} \mathbf{x}_2^\top \tilde{\mathbf{B}}_{(-2)}^{-1} \mathbf{x}_2 &= \mathbf{z}_1^\top (\mathbf{B}_{(-1)} + (\sigma_1^2 - \sigma_2^2) \mathbf{z}_2 \mathbf{z}_2^\top)^{-1} \mathbf{z}_1 \\ &= \mathbf{z}_1^\top \mathbf{B}_{(-1)}^{-1} \mathbf{z}_1 - \frac{(\sigma_1^2 - \sigma_2^2) \mathbf{z}_1^\top \mathbf{B}_{(-1)}^{-1} \mathbf{z}_2 \mathbf{z}_2^\top \mathbf{B}_{(-1)}^{-1} \mathbf{z}_1}{1 + \mathbf{z}_2^\top \mathbf{B}_{(-1)}^{-1} \mathbf{z}_2} \leq \mathbf{z}_1^\top \mathbf{B}_{(-1)}^{-1} \mathbf{z}_1. \end{aligned}$$

The equality holds only when  $\mathbf{z}_1^\top \mathbf{B}_{(-1)}^{-1} \mathbf{z}_2 = 0$ , which happens with zero probability. In the following, we will then only consider the case that  $\mathbf{x}_2^\top \tilde{\mathbf{B}}_{(-2)}^{-1} \mathbf{x}_2 < \mathbf{z}_1^\top \mathbf{B}_{(-1)}^{-1} \mathbf{z}_1$ , which holds with probability one. Since  $\sigma_1 > \sigma_2 > 0$ , we have  $\sigma_2^2 \mathbf{x}_2^\top \tilde{\mathbf{B}}_{(-2)}^{-1} \mathbf{x}_2 < \sigma_1^2 \mathbf{z}_1^\top \mathbf{B}_{(-1)}^{-1} \mathbf{z}_1$ . Along with (A.3), we have

$$\sigma_2^2 \mathbf{x}_2^\top \left( \sum_{l=1}^m \sigma_l^2 \mathbf{x}_l \mathbf{x}_l^\top \right)^{-1} \mathbf{x}_2 < \sigma_1^2 \mathbf{z}_1^\top \left( \sum_{l=1}^m \sigma_l^2 \mathbf{z}_l \mathbf{z}_l^\top \right)^{-1} \mathbf{z}_1.$$

Similarly, we have  $\sigma_1^2 \mathbf{x}_1^\top \left( \sum_{l=1}^m \sigma_l^2 \mathbf{x}_l \mathbf{x}_l^\top \right)^{-1} \mathbf{x}_1 > \sigma_2^2 \mathbf{z}_2^\top \left( \sum_{l=1}^m \sigma_l^2 \mathbf{z}_l \mathbf{z}_l^\top \right)^{-1} \mathbf{z}_2$ . Then,

$$\begin{aligned} &\sigma_1^2 \mathbf{z}_1^\top \left( \sum_{l=1}^m \sigma_l^2 \mathbf{z}_l \mathbf{z}_l^\top \right)^{-1} \mathbf{z}_1 + \sigma_1^2 \mathbf{x}_1^\top \left( \sum_{l=1}^m \sigma_l^2 \mathbf{x}_l \mathbf{x}_l^\top \right)^{-1} \mathbf{x}_1 \\ &> \sigma_2^2 \mathbf{x}_2^\top \left( \sum_{l=1}^m \sigma_l^2 \mathbf{x}_l \mathbf{x}_l^\top \right)^{-1} \mathbf{x}_2 + \sigma_2^2 \mathbf{z}_2^\top \left( \sum_{l=1}^m \sigma_l^2 \mathbf{z}_l \mathbf{z}_l^\top \right)^{-1} \mathbf{z}_2. \end{aligned}$$

Take the expectation, and we have

$$\begin{aligned} &E \left( \sigma_1^2 \mathbf{z}_1^\top \left( \sum_{l=1}^m \sigma_l^2 \mathbf{z}_l \mathbf{z}_l^\top \right)^{-1} \mathbf{z}_1 \right) + E \left( \sigma_1^2 \mathbf{x}_1^\top \left( \sum_{l=1}^m \sigma_l^2 \mathbf{x}_l \mathbf{x}_l^\top \right)^{-1} \mathbf{x}_1 \right) \\ &> E \left( \sigma_2^2 \mathbf{x}_2^\top \left( \sum_{l=1}^m \sigma_l^2 \mathbf{x}_l \mathbf{x}_l^\top \right)^{-1} \mathbf{x}_2 \right) + E \left( \sigma_2^2 \mathbf{z}_2^\top \left( \sum_{l=1}^m \sigma_l^2 \mathbf{z}_l \mathbf{z}_l^\top \right)^{-1} \mathbf{z}_2 \right). \quad (\text{A.4}) \end{aligned}$$

Since  $\tilde{\boldsymbol{\Omega}}_{[i]}$  and  $\boldsymbol{\Omega}_{[i]}$  have the same distribution, we have  $\boldsymbol{\Omega}_{[i]}^\top \mathbf{V} \stackrel{d}{=} \tilde{\boldsymbol{\Omega}}_{[i]}^\top \mathbf{V} = \boldsymbol{\Omega}_{[i]}^\top \mathbf{V}_{1,2}$ , and hence  $[\mathbf{z}_1, \mathbf{z}_2, \mathbf{z}_3, \dots, \mathbf{z}_n] \stackrel{d}{=} [\mathbf{x}_1, \mathbf{x}_2, \mathbf{x}_3, \dots, \mathbf{x}_n]$ . Then,

$$\begin{aligned} E \left( \sigma_1^2 \mathbf{z}_1^\top \left( \sum_{l=1}^m \sigma_l^2 \mathbf{z}_l \mathbf{z}_l^\top \right)^{-1} \mathbf{z}_1 \right) &= E \left( \sigma_1^2 \mathbf{x}_1^\top \left( \sum_{l=1}^m \sigma_l^2 \mathbf{x}_l \mathbf{x}_l^\top \right)^{-1} \mathbf{x}_1 \right) \\ E \left( \sigma_2^2 \mathbf{x}_2^\top \left( \sum_{l=1}^m \sigma_l^2 \mathbf{x}_l \mathbf{x}_l^\top \right)^{-1} \mathbf{x}_2 \right) &= E \left( \sigma_2^2 \mathbf{z}_2^\top \left( \sum_{l=1}^m \sigma_l^2 \mathbf{z}_l \mathbf{z}_l^\top \right)^{-1} \mathbf{z}_2 \right). \end{aligned}$$

Therefore, (A.4) becomes

$$E \left\{ \sigma_1^2 \mathbf{z}_1^\top \left( \sum_{l=1}^m \sigma_l^2 \mathbf{z}_l \mathbf{z}_l^\top \right)^{-1} \mathbf{z}_1 \right\} > E \left\{ \sigma_2^2 \mathbf{z}_2^\top \left( \sum_{l=1}^m \sigma_l^2 \mathbf{z}_l \mathbf{z}_l^\top \right)^{-1} \mathbf{z}_2 \right\}. \quad (\text{A.5})$$

Similarly, we can have  $E \left( \sigma_j^2 \mathbf{z}_j^\top \left( \sum_{l=1}^m \sigma_l^2 \mathbf{z}_l \mathbf{z}_l^\top \right)^{-1} \mathbf{z}_j \right) > E \left( \sigma_{j'}^2 \mathbf{z}_{j'}^\top \left( \sum_{l=1}^m \sigma_l^2 \mathbf{z}_l \mathbf{z}_l^\top \right)^{-1} \mathbf{z}_{j'} \right)$  for any pair of  $(j, j')$  satisfying  $j < j'$ .  $\square$

**A.2. Proof of Theorem 2.2.** *Proof.* Direct calculations lead to the following equalities for  $\mathbf{Q} \in \mathcal{S}_{m,\ell}$ :

$$\begin{aligned} & \left\| \mathbf{Q}_{[i]} \mathbf{Q}_{[i]}^\top - \mathbf{Q} \mathbf{Q}^\top \right\|_F^2 = \text{tr} \left\{ (\mathbf{Q}_{[i]} \mathbf{Q}_{[i]}^\top - \mathbf{Q} \mathbf{Q}^\top)^2 \right\} \\ & = \text{tr} \left\{ \mathbf{Q}_{[i]} \mathbf{Q}_{[i]}^\top \right\} + \text{tr} \left\{ \mathbf{Q} \mathbf{Q}^\top \right\} - 2 \text{tr} \left\{ \mathbf{Q}_{[i]} \mathbf{Q}_{[i]}^\top \mathbf{Q} \mathbf{Q}^\top \right\} \\ & = 2\ell - 2 \text{tr} \left\{ \mathbf{Q} \mathbf{Q}^\top \mathbf{Q}_{[i]} \mathbf{Q}_{[i]}^\top \right\}. \end{aligned}$$

Hence the summation becomes  $\sum_{i=1}^N \left\| \mathbf{Q}_{[i]} \mathbf{Q}_{[i]}^\top - \mathbf{Q} \mathbf{Q}^\top \right\|_F^2 = 2N\ell - 2N \text{tr}(\mathbf{Q} \mathbf{Q}^\top \bar{\mathbf{P}})$ . Similarly, one can also show that  $\left\| \bar{\mathbf{P}} - \mathbf{Q} \mathbf{Q}^\top \right\|_F^2 = \text{tr}(\bar{\mathbf{P}}^2) + \ell - 2 \text{tr}(\mathbf{Q} \mathbf{Q}^\top \bar{\mathbf{P}})$ . Since  $\ell$  and  $\bar{\mathbf{P}}$  are given and fixed, the two optimization problems are equivalent.  $\square$

**A.3. Proof of Theorem 3.1.** Note that the optimization in Stiefel manifold has been analyzed in [22, 23]. Here we derive the related properties by using fundamental matrix algebras and calculus. We hope this approach based on fundamental tools may benefit readers who are not familiar with the advanced differential geometry topics adopted in [22, 23].

*Proof.* First we find a necessary and sufficient condition for  $\mathbf{X}$  being in  $\mathcal{T}_{\mathbf{Q}} \mathcal{S}_{m,\ell}$ . For all  $\mathbf{X} \in \mathcal{T}_{\mathbf{Q}} \mathcal{S}_{m,\ell}$ , find a path  $\Gamma(t)$  in  $\mathcal{S}_{m,\ell}$  with  $\Gamma(0) = \mathbf{Q}$  and  $\Gamma'(0) = \mathbf{X}$ . From  $\Gamma(t)^\top \Gamma(t) = \mathbf{I}$ , differentiate each side by  $t$  and take  $t = 0$ , we have

$$\mathbf{X}^\top \mathbf{Q} + \mathbf{Q}^\top \mathbf{X} = \mathbf{0}, \quad (\text{A.6})$$

which gives a necessary condition for  $\mathbf{X} \in \mathcal{T}_{\mathbf{Q}} \mathcal{S}_{m,\ell}$ . There are  $\ell(\ell + 1)/2$  conditions for  $\mathbf{X}$  in (A.6) and the dimension of  $\mathcal{T}_{\mathbf{Q}} \mathcal{S}_{m,\ell}$  is  $m\ell - \ell(\ell + 1)/2$ , which means (A.6) is also a sufficient condition for  $\mathbf{X} \in \mathcal{T}_{\mathbf{Q}} \mathcal{S}_{m,\ell}$ . By taking vec to each sides of (A.6), we get the equality

$$[(\mathbf{Q}^\top \otimes \mathbf{I}_\ell) \mathbf{K}_{m,\ell} + (\mathbf{I}_\ell \otimes \mathbf{Q}^\top)] \text{vec}(\mathbf{X}) = \mathbf{0},$$

where  $\otimes$  denotes the Kronecker product and  $\mathbf{K}_{m,\ell}$  denotes the  $m \times \ell$  commutation matrix [13]. Define  $\mathbf{T} = \mathbf{K}_{\ell,m} (\mathbf{Q} \otimes \mathbf{I}_\ell) + (\mathbf{I}_\ell \otimes \mathbf{Q})$  and get  $\mathbf{T}^\top \text{vec}(\mathbf{X}) = \mathbf{0}$ . This shows that the tangent space (after vectorizing each elements) is contained in the null space of  $\mathbf{T}^\top$ . One can compute the rank of  $\mathbf{T}$  and shows that the null space of  $\mathbf{T}^\top$  is actually the tangent space. Hence the projection matrix onto the tangent space is given by  $(\mathbf{I} - \mathbf{P}_{\mathbf{T}})$ , where  $\mathbf{P}_{\mathbf{T}} = \mathbf{T}(\mathbf{T}^\top \mathbf{T})^+ \mathbf{T}^\top$  and  $(\mathbf{T}^\top \mathbf{T})^+$  denoted the Moore-Penrose pseudo-inverse. With  $\mathbf{P}_{\mathbf{T}}$ ,  $\mathbf{D}_F$  can be given via  $\text{vec}(\mathbf{D}_F) = (\mathbf{I} - \mathbf{P}_{\mathbf{T}}) \text{vec}(\mathbf{G}_F)$ . With some calculation, we have  $\mathbf{T} = (\mathbf{I}_\ell \otimes \mathbf{Q})(\mathbf{I}_{\ell^2} + \mathbf{K}_{\ell,\ell})$  and thus

$$\begin{aligned} \mathbf{T}^\top \mathbf{T} &= (\mathbf{I}_{\ell^2} + \mathbf{K}_{\ell,\ell})^\top (\mathbf{I}_\ell \otimes \mathbf{Q})^\top (\mathbf{I}_\ell \otimes \mathbf{Q})(\mathbf{I}_{\ell^2} + \mathbf{K}_{\ell,\ell}) \\ &= (\mathbf{I}_{\ell^2} + \mathbf{K}_{\ell,\ell})(\mathbf{I}_{\ell^2} + \mathbf{K}_{\ell,\ell}) = 2(\mathbf{I}_{\ell^2} + \mathbf{K}_{\ell,\ell}). \end{aligned}$$

Then the projection matrix  $\mathbf{P}_T$  can be calculated as:

$$\begin{aligned} \mathbf{P}_T &= \mathbf{T}(\mathbf{T}^\top \mathbf{T})^+ \mathbf{T}^\top \\ &= (\mathbf{I}_\ell \otimes \mathbf{Q})(\mathbf{I}_{\ell^2} + \mathbf{K}_{\ell, \ell}) \frac{1}{2} (\mathbf{I}_{\ell^2} + \mathbf{K}_{\ell, \ell})^+ (\mathbf{I}_{\ell^2} + \mathbf{K}_{\ell, \ell})^\top (\mathbf{I}_\ell \otimes \mathbf{Q})^\top \\ &= \frac{1}{2} (\mathbf{I}_\ell \otimes \mathbf{Q})(\mathbf{I}_{\ell^2} + \mathbf{K}_{\ell, \ell})(\mathbf{I}_\ell \otimes \mathbf{Q}^\top) \frac{1}{2} (\mathbf{I}_\ell \otimes \mathbf{Q}\mathbf{Q}^\top) + \frac{1}{2} (\mathbf{Q}^\top \otimes \mathbf{Q}) \mathbf{K}_{m, \ell}. \end{aligned}$$

Hence, by  $\text{vec}(\mathbf{D}_F) = (\mathbf{I} - \mathbf{P}_T) \text{vec}(\mathbf{G}_F)$ ,

$$\begin{aligned} \text{vec}(\mathbf{D}_F) &= (\mathbf{I}_{\ell^2} - \frac{1}{2} (\mathbf{I}_\ell \otimes \mathbf{Q}\mathbf{Q}^\top) - \frac{1}{2} (\mathbf{Q}^\top \otimes \mathbf{Q}) \mathbf{K}_{m, \ell}) \text{vec}(\mathbf{G}_F) \\ &= \text{vec}(\mathbf{G}_F) - \frac{1}{2} (\mathbf{I}_\ell \otimes \mathbf{Q}\mathbf{Q}^\top) \text{vec}(\mathbf{G}_F) - \frac{1}{2} (\mathbf{Q}^\top \otimes \mathbf{Q}) \mathbf{K}_{m, \ell} \text{vec}(\mathbf{G}_F) \\ &= \text{vec}(\mathbf{G}_F) - \frac{1}{2} \text{vec}(\mathbf{Q}\mathbf{Q}^\top \mathbf{G}_F) - \frac{1}{2} \text{vec}(\mathbf{Q}\mathbf{G}_F^\top \mathbf{Q}) \end{aligned}$$

and  $\mathbf{D}_F$  can be written as

$$\mathbf{D}_F = \left( \mathbf{I} - \frac{1}{2} \mathbf{Q}\mathbf{Q}^\top \right) \mathbf{G}_F - \frac{1}{2} \mathbf{Q}\mathbf{G}_F^\top \mathbf{Q}. \quad (\text{A.7})$$

Since we have the property  $\mathbf{Q}^\top \mathbf{G}_F(\mathbf{Q}) = \mathbf{G}_F(\mathbf{Q})^\top \mathbf{Q}$  here, we can get  $\mathbf{D}_F(\mathbf{Q}) = (\mathbf{I} - \mathbf{Q}\mathbf{Q}^\top) \mathbf{G}_F(\mathbf{Q})$ . This completes the proof.  $\square$

**A.4. Proof of Lemma 3.2.** *Proof.* (a) Express  $\mathbf{W}$  as  $\mathbf{Q}\mathbf{C} + \mathbf{Q}_\perp \mathbf{B}$ . Then,  $\mathbf{W}^\top \mathbf{W} = \mathbf{I}$  will imply  $\mathbf{C}^2 + \mathbf{B}^\top \mathbf{B} = \mathbf{I}$ . Thus,  $\mathbf{C}^4 + \mathbf{C}\mathbf{B}^\top \mathbf{B}\mathbf{C} = \mathbf{C}^2$ . Furthermore,  $\varphi_{\mathbf{Q}}(\mathbf{W}) = (\mathbf{I} - \mathbf{Q}\mathbf{Q}^\top) \mathbf{W}\mathbf{W}^\top \mathbf{Q} = \mathbf{Q}_\perp \mathbf{B}\mathbf{C}$ . Then, we have

$$\frac{\mathbf{I}}{4} - \varphi_{\mathbf{Q}}(\mathbf{W})^\top \varphi_{\mathbf{Q}}(\mathbf{W}) = \frac{\mathbf{I}}{4} - \mathbf{C}\mathbf{B}^\top \mathbf{B}\mathbf{C} = \frac{\mathbf{I}}{4} - \mathbf{C}^2 + \mathbf{C}^4 = \left( \frac{\mathbf{I}}{2} - \mathbf{C}^2 \right)^2,$$

which is non-negative definite. (b) Let  $\mathbf{X}_{[i]} = (\mathbf{I} - \mathbf{Q}\mathbf{Q}^\top) \mathbf{Q}_{[i]} \mathbf{Q}_{[i]}^\top \mathbf{Q}$ . Then, for any vector  $\mathbf{v} \in \mathbb{R}^\ell$

$$\begin{aligned} \mathbf{v}^\top \left( \frac{\mathbf{I}}{4} - \mathbf{X}^\top \mathbf{X} \right) \mathbf{v} &= \frac{\|\mathbf{v}\|^2}{4} - \left\| \frac{1}{N} \sum_{i=1}^N \mathbf{X}_{[i]} \mathbf{v} \right\|^2 \\ &\geq \frac{\|\mathbf{v}\|^2}{4} - \frac{1}{N} \sum_{i=1}^N \|\mathbf{X}_{[i]} \mathbf{v}\|^2 = \frac{1}{N} \sum_{i=1}^N \left( \frac{1}{4} \|\mathbf{v}\|^2 - \|\mathbf{X}_{[i]} \mathbf{v}\|^2 \right) \geq 0. \end{aligned}$$

The last inequality holds since  $\|\mathbf{X}_{[i]} \mathbf{v}\| \leq \|\mathbf{v}\|/2$  for every  $i$  from (a).  $\square$

**A.5. Proof of Lemma 3.3.** *Proof.* We will show this lemma under the condition that  $\mathbf{X}$  has full rank. For  $\mathbf{X}$  being rank deficient, the proof is more complicated and is placed in Appendix A.7. Express  $\mathbf{W} = \mathbf{Q}\mathbf{C} + \mathbf{Q}_\perp \mathbf{B}$ . We want to find  $\mathbf{B}$  and  $\mathbf{C}$  satisfying (a)  $\mathbf{W}^\top \mathbf{W} = \mathbf{I}_\ell$  and (b)  $\mathbf{X} = \varphi_{\mathbf{Q}}(\mathbf{W})$ . From condition (b), it leads to  $\mathbf{X} = (\mathbf{I} - \mathbf{Q}\mathbf{Q}^\top) (\mathbf{Q}\mathbf{C} + \mathbf{Q}_\perp \mathbf{B}) (\mathbf{Q}\mathbf{C} + \mathbf{Q}_\perp \mathbf{B})^\top \mathbf{Q} = \mathbf{Q}_\perp \mathbf{B}\mathbf{C}$ . Since  $\mathbf{X}$  has full rank,  $\mathbf{C}$  has to have full rank and hence is invertible. Then,  $\mathbf{Q}_\perp \mathbf{B} = \mathbf{X}\mathbf{C}^{-1}$ . From condition (a), it leads to  $\mathbf{I} = (\mathbf{Q}\mathbf{C} + \mathbf{Q}_\perp \mathbf{B})^\top (\mathbf{Q}\mathbf{C} + \mathbf{Q}_\perp \mathbf{B}) = \mathbf{C}^2 + \mathbf{C}^{-1} \mathbf{X}^\top \mathbf{X} \mathbf{C}^{-1}$ . Then,  $\mathbf{C}^2 = \mathbf{C}^4 + \mathbf{X}^\top \mathbf{X}$ . With the assumption that  $\frac{\mathbf{I}}{4} - \mathbf{X}^\top \mathbf{X}$  is non-negative definite, we have  $\left\{ \mathbf{C}^2 - \frac{\mathbf{I}}{2} \right\}^2 = \frac{\mathbf{I}}{4} - \mathbf{X}^\top \mathbf{X}$ , and then  $\mathbf{C} = \left\{ \frac{\mathbf{I}}{2} + \left( \frac{\mathbf{I}}{4} - \mathbf{X}^\top \mathbf{X} \right)^{1/2} \right\}^{1/2}$ .  $\square$



**A.6. Matrix Square Root.** A matrix square root for a symmetric and non-negative definite matrix  $M \in \mathbb{R}^{\ell \times \ell}$  is defined as follows.

$$M^{1/2} \text{ is any matrix } T \text{ that satisfies } TT^\top = M. \quad (\text{A.8})$$

Express  $M$  in its spectrum  $M = \mathbf{G}D\mathbf{G}^\top$ . If we restrict  $T$  to be symmetric, then

$$T = \mathbf{G}D^{1/2}\mathbf{G}^\top, \text{ where } D^{1/2} = \text{diag}([\pm\sqrt{d_1}, \dots, \pm\sqrt{d_\ell}]). \quad (\text{A.9})$$

If  $T$  is further restricted to be non-negative definite, then it is uniquely given by

$$T = \mathbf{G}D^{1/2}\mathbf{G}^\top, \text{ where } D^{1/2} = \text{diag}([\sqrt{d_1}, \dots, \sqrt{d_\ell}]). \quad (\text{A.10})$$

**A.7. Proof of Lemma 3.3 for Rank Deficient  $X$ .** *Proof.* Let  $\mathbf{W} = \mathbf{Q}\mathbf{C} + \mathbf{X}\mathbf{B}$ . It suffices to show that  $\mathbf{C}$  is nonsingular. Then we have  $\mathbf{X}\mathbf{B} = \mathbf{X}\mathbf{C}^{-1}$  again, and the rest arguments of the proof for Lemma 3.3 remain the same. If  $\mathbf{C}\mathbf{v} = \mathbf{0}$  for some nonzero column vector  $\mathbf{v}$ , we have  $\mathbf{X}\mathbf{v} = \mathbf{X}\mathbf{B}\mathbf{C}\mathbf{v} = \mathbf{0}$ . Factorize  $\mathbf{C}$  as

$$\mathbf{C} = [\mathbf{T}_1, \mathbf{T}_2]_{\ell \times \ell} \begin{bmatrix} D_{\ell_1 \times \ell_1} & \mathbf{0}_{\ell_1 \times (\ell - \ell_1)} \\ \mathbf{0}_{(\ell - \ell_1) \times \ell_1} & \mathbf{0}_{(\ell - \ell_1) \times (\ell - \ell_1)} \end{bmatrix} \begin{bmatrix} \mathbf{T}_1^\top \\ \mathbf{T}_2^\top \end{bmatrix}_{\ell \times \ell},$$

where  $D$  is diagonal and nonsingular, and  $[\mathbf{T}_1, \mathbf{T}_2]^\top [\mathbf{T}_1, \mathbf{T}_2] = \mathbf{I}$ . Since  $\mathbf{C}\mathbf{T}_2 = \mathbf{0}$ , so is  $\mathbf{X}\mathbf{T}_2$ , which means that  $\mathbf{X}$  can be factorized as  $\mathbf{X} = \mathbf{Y} [\widetilde{\mathbf{X}}_{m \times \ell_1}, \mathbf{0}_{m \times (\ell - \ell_1)}] \mathbf{T}^\top$  where  $\mathbf{T} = [\mathbf{T}_1, \mathbf{T}_2]$ , and  $\mathbf{Y}^\top \mathbf{Y} = \mathbf{I}$ . Let  $\widetilde{\mathbf{B}} = \mathbf{T}^\top \mathbf{B}\mathbf{T}$ . (b) leads to

$$\mathbf{Y} [\widetilde{\mathbf{X}}_{m \times \ell_1}, \mathbf{0}_{m \times (\ell - \ell_1)}] = \mathbf{Y} [\widetilde{\mathbf{X}}_{m \times \ell_1}, \mathbf{0}_{m \times (\ell - \ell_1)}] \widetilde{\mathbf{B}} \begin{bmatrix} D_{\ell_1 \times \ell_1} & \mathbf{0}_{\ell_1 \times (\ell - \ell_1)} \\ \mathbf{0}_{(\ell - \ell_1) \times \ell_1} & \mathbf{0}_{(\ell - \ell_1) \times (\ell - \ell_1)} \end{bmatrix},$$

which forces  $\widetilde{\mathbf{B}}$  to be of the form  $\widetilde{\mathbf{B}} = \begin{bmatrix} \widetilde{\mathbf{B}}_{11} & \widetilde{\mathbf{B}}_{12} \\ \widetilde{\mathbf{B}}_{21} & \widetilde{\mathbf{B}}_{22} \end{bmatrix}$  with  $\widetilde{\mathbf{X}}_{m \times \ell_1} \widetilde{\mathbf{B}}_{11} = \widetilde{\mathbf{X}}_{m \times \ell_1} D^{-1}$ .

Then

$$\mathbf{B}^\top \mathbf{X}^\top \mathbf{X} \mathbf{B} = \mathbf{T} \begin{bmatrix} D^{-1} \widetilde{\mathbf{X}}^\top \widetilde{\mathbf{X}} D^{-1} & D^{-1} \widetilde{\mathbf{X}}^\top \widetilde{\mathbf{X}} \widetilde{\mathbf{B}}_{12} \\ \widetilde{\mathbf{B}}_{12}^\top \widetilde{\mathbf{X}}^\top \widetilde{\mathbf{X}} D^{-1} & \widetilde{\mathbf{B}}_{12}^\top \widetilde{\mathbf{X}}^\top \widetilde{\mathbf{X}} \widetilde{\mathbf{B}}_{12} \end{bmatrix} \mathbf{T}^\top.$$

(a) leads to  $D^{-1} \widetilde{\mathbf{X}}^\top \widetilde{\mathbf{X}} \widetilde{\mathbf{B}}_{12} = \mathbf{0}$  and  $\widetilde{\mathbf{B}}_{12}^\top \widetilde{\mathbf{X}}^\top \widetilde{\mathbf{X}} \widetilde{\mathbf{B}}_{12} = \mathbf{I}$ , which contradicts to each other. Therefore,  $\mathbf{C}$  has to be nonsingular.  $\square$

**A.8. Proof of Theorem 3.5.** Since  $\Omega_{[i]}$ 's consist of all i.i.d. Gaussian entries, we have that  $\overline{\mathbf{P}}$  has distinct eigenvalues almost surely. Let the eigenvalue decomposition of  $\overline{\mathbf{P}}$  be denoted by  $\overline{\mathbf{P}} = [\mathbf{Q}_* \quad \mathbf{Q}_\perp] \begin{bmatrix} \Lambda_1 & \mathbf{0} \\ \mathbf{0} & \Lambda_2 \end{bmatrix} [\mathbf{Q}_* \quad \mathbf{Q}_\perp]^\top$ , where  $\Lambda_1 = \text{diag}([\lambda_1, \dots, \lambda_\ell])$  and  $\Lambda_2 = \text{diag}([\lambda_{\ell+1}, \dots, \lambda_m])$ .

*Proof.* Suppose we start from an initial  $\mathbf{Q}_{\text{ini}} \in \mathcal{N}_\varepsilon(\mathbf{Q}_* \mathbf{R}_0)$ , where  $\mathbf{R}_0$  is an arbitrary orthogonal matrix and  $\varepsilon$  is determined later. Denote  $\mathbf{Q}_0 := \mathbf{Q}_{\text{ini}}$  and  $\mathbf{Q}_{t+1} := g(\mathbf{Q}_t)$ , where  $g$  is defined in (3.11). We can write  $\mathbf{Q}_0$  as  $\mathbf{Q}_0 = \mathbf{Q}_* \mathbf{R}_0 \mathbf{C}_{0,1} + \mathbf{Q}_\perp \mathbf{C}_{0,2}$ , where  $\mathbf{C}_{0,1} \in \mathbb{R}^{\ell \times \ell}$ ,  $\mathbf{C}_{0,2} \in \mathbb{R}^{(m-\ell) \times \ell}$  and  $\mathbf{C}_{0,1}^\top \mathbf{C}_{0,1} + \mathbf{C}_{0,2}^\top \mathbf{C}_{0,2} = \mathbf{I}_\ell$ . We first show that  $\mathbf{R}_{0,*}^\top \mathbf{R}_0 \mathbf{C}_{0,1}$  is symmetric, where

$$\mathbf{R}_{0,*} := \underset{\mathbf{R} \in \mathcal{S}_{\ell, \ell}}{\text{argmin}} \|\mathbf{Q}_0 - \mathbf{Q}_* \mathbf{R}\|_F = \underset{\mathbf{R} \in \mathcal{S}_{\ell, \ell}}{\text{argmin}} \|\mathbf{Q}_* \mathbf{R}_0 \mathbf{C}_{0,1} - \mathbf{Q}_* \mathbf{R}\|_F = \underset{\mathbf{R} \in \mathcal{S}_{\ell, \ell}}{\text{argmin}} \|\mathbf{C}_{0,1} - \mathbf{R}_0^\top \mathbf{R}\|_F.$$

Denote the spectrum of  $\mathbf{C}_{0,1}$  as  $\mathbf{C}_{0,1} = \mathbf{L}\mathbf{S}\mathbf{H}^\top$ , where the diagonal entries of  $\mathbf{S}$  are less than or equal to one. Therefore, the best approximation is given by  $\mathbf{R}_0^\top \mathbf{R}_{0,*} = \mathbf{L}\mathbf{H}^\top$ . Then,  $\mathbf{R}_{0,*}^\top \mathbf{R}_0 \mathbf{C}_{0,1} = \mathbf{H}\mathbf{L}^\top \mathbf{L}\mathbf{S}\mathbf{H}^\top = \mathbf{H}\mathbf{S}\mathbf{H}^\top$ . This completes the proof of symmetry. With this symmetry property, we can write  $\mathbf{Q}_0$  as  $\mathbf{Q}_0 = \mathbf{Q}_* \mathbf{R}_{0,*} \mathbf{C}_1 + \mathbf{Q}_\perp \mathbf{C}_2$  for some symmetric  $\mathbf{C}_1 \in \mathbb{R}^{\ell \times \ell}$  and some  $\mathbf{C}_2 \in \mathbb{R}^{(m-\ell) \times \ell}$ .

Next, we (i) extend the definition of  $g$  to an open covering  $\mathcal{O}_{\varepsilon_0}$  of the compact Stiefel manifold  $\mathcal{S}_{m \times \ell}$  for some small  $\varepsilon_0 > 0$ . (ii) Compute its derivative (the usual derivative in the Euclidean space)  $\mathbf{D}(\mathbf{Q}_* \mathbf{R}_{0,*}) := \partial \text{vec}(g) / \partial \text{vec}(\mathbf{M})^\top \big|_{\mathbf{M}=\mathbf{Q}_* \mathbf{R}_{0,*}}$ , where  $\mathbf{M} \in \mathcal{O}_{\varepsilon_0}$ . (iii) Show that  $\mathbf{D}$ 's spectral norm, when restricted to the subspace  $\mathcal{V}_0$  given below (A.11), is strictly less than one. (iv)  $\|\text{vec}(\mathbf{Q}_1) - \text{vec}(\mathbf{Q}_* \mathbf{R}_{0,*})\|_2 \leq \sqrt{\alpha} \|\text{vec}(\mathbf{Q}_0) - \text{vec}(\mathbf{Q}_* \mathbf{R}_{0,*})\|_2$  for some  $0 \leq \alpha < 1$ . (v)  $\|\text{vec}(\mathbf{Q}_1) - \text{vec}(\mathbf{Q}_* \mathbf{R}_{1,*})\|_2 \leq \sqrt{\alpha} \|\text{vec}(\mathbf{Q}_0) - \text{vec}(\mathbf{Q}_* \mathbf{R}_{0,*})\|_2$ , where  $\mathbf{R}_{1,*}$  is defined below (A.12). (vi) Iteratively obtain  $\|\text{vec}(\mathbf{Q}_{t+1}) - \text{vec}(\mathbf{Q}_* \mathbf{R}_{t+1,*})\|_2 \leq \alpha^{(t+1)/2} \|\text{vec}(\mathbf{Q}_0) - \text{vec}(\mathbf{Q}_* \mathbf{R}_{0,*})\|_2$ . (vii) Finally, establish the convergence of  $\mathbf{Q}_t$ .

(i) For  $\varepsilon_0$  sufficiently small, matrices  $\mathbf{C}(\mathbf{Q})$  and  $\mathbf{X}(\mathbf{Q})$  as functions of  $\mathbf{Q}$  can be extended to an open covering  $\mathcal{O}_{\varepsilon_0} := \{\mathbf{M} \in \mathbb{R}^{m \times \ell} : \inf_{\mathbf{Q} \in \mathcal{S}_{m,\ell}} \|\mathbf{M} - \mathbf{Q}\|_F < \varepsilon_0\}$  of the compact Stiefel manifold  $\mathcal{S}_{m \times \ell}$ . Then,  $g$  can be extended as well. From now on, we consider  $g$  as a function defined on this open covering  $\mathcal{O}_{\varepsilon_0}$  and we can take derivative of  $g$  in the usual Euclidean sense.

(ii) Recall  $\mathbf{X}(\mathbf{Q}) = (\mathbf{I} - \mathbf{Q}\mathbf{Q}^\top) \overline{\mathbf{P}} \mathbf{Q}$ ,  $\mathbf{C} = \left\{ \frac{\mathbf{I}}{2} + \left( \frac{\mathbf{I}}{4} - \mathbf{X}^\top \mathbf{X} \right)^{1/2} \right\}^{1/2}$ , and  $\mathbf{C}$  satisfies the equation  $\mathbf{C}^4 - \mathbf{C}^2 + \mathbf{X}^\top \mathbf{X} = \mathbf{0}$ . By taking derivative for both sides of the last equation, we have  $\frac{\partial \text{vec}(\mathbf{C}^4 - \mathbf{C}^2 + \mathbf{X}^\top \mathbf{X})}{\partial \text{vec}(\mathbf{Q})^\top} \big|_{\mathbf{Q}_* \mathbf{R}_{0,*}} = \mathbf{0}$ . The left side of the equation can be calculated as follows.

$$\begin{aligned} & \left\{ \mathbf{C}^3 \otimes \mathbf{I} + \mathbf{C}^2 \otimes \mathbf{C} + \mathbf{C} \otimes \mathbf{C}^2 + \mathbf{I} \otimes \mathbf{C}^3 - \mathbf{C} \otimes \mathbf{I} - \mathbf{I} \otimes \mathbf{C} \right\} \frac{\partial \text{vec}(\mathbf{C})}{\partial \text{vec}(\mathbf{Q})^\top} \\ & + \left\{ \mathbf{I} \otimes \mathbf{X}^\top + (\mathbf{X}^\top \otimes \mathbf{I}) \mathbf{K}_{m,\ell} \right\} \frac{\partial \text{vec}(\mathbf{X})}{\partial \text{vec}(\mathbf{Q})^\top} \bigg|_{\mathbf{Q}_* \mathbf{R}_{0,*}} = \frac{2 \partial \text{vec}(\mathbf{C})}{\partial \text{vec}(\mathbf{Q})^\top} \bigg|_{\mathbf{Q}_* \mathbf{R}_{0,*}}, \end{aligned}$$

where the equality holds by the facts  $\mathbf{X}(\mathbf{Q}_* \mathbf{R}_{0,*}) = \mathbf{0}$  and  $\mathbf{C}(\mathbf{Q}_* \mathbf{R}_{0,*}) = \mathbf{I}$ . Hence, we have  $\frac{\partial \text{vec}(\mathbf{C})}{\partial \text{vec}(\mathbf{Q})^\top} \big|_{\mathbf{Q}_* \mathbf{R}_{0,*}} = \mathbf{0}$ . Applying similar techniques to both sides of the equation  $g(\mathbf{Q})\mathbf{C} = \mathbf{Q}\mathbf{C}^2 + \mathbf{X}$ , we get

$$\frac{\partial \text{vec}(g)}{\partial \text{vec}(\mathbf{Q})^\top} \bigg|_{\mathbf{Q}_* \mathbf{R}_{0,*}} = \mathbf{I}_{m\ell} + \frac{\partial \mathbf{X}}{\partial \text{vec}(\mathbf{Q})^\top} \bigg|_{\mathbf{Q}_* \mathbf{R}_{0,*}}.$$

Some further calculation goes as follows.

$$\begin{aligned} \mathbf{D}(\mathbf{Q}_* \mathbf{R}_{0,*}) &= \mathbf{I}_{m\ell} + \frac{\partial \text{vec}(\mathbf{X})}{\partial \text{vec}(\mathbf{Q})^\top} \bigg|_{\mathbf{Q}_* \mathbf{R}_{0,*}} = \mathbf{I}_{m\ell} + \frac{\partial \text{vec}((\mathbf{I} - \mathbf{Q}\mathbf{Q}^\top) \overline{\mathbf{P}} \mathbf{Q})}{\partial \text{vec}(\mathbf{Q})^\top} \bigg|_{\mathbf{Q}_* \mathbf{R}_{0,*}} \\ &= \mathbf{I}_{m\ell} + \mathbf{I}_\ell \otimes \overline{\mathbf{P}} - \mathbf{Q}^\top \overline{\mathbf{P}} \mathbf{Q} \otimes \mathbf{I}_m - (\mathbf{Q}^\top \overline{\mathbf{P}} \otimes \mathbf{Q}) \mathbf{K}_{m,\ell} - \mathbf{I}_\ell \otimes \mathbf{Q}\mathbf{Q}^\top \overline{\mathbf{P}} \bigg|_{\mathbf{Q}_* \mathbf{R}_{0,*}} \\ &= \mathbf{I}_{m\ell} + \mathbf{I}_\ell \otimes \overline{\mathbf{P}} - \mathbf{R}_{0,*}^\top \Lambda_1 \mathbf{R}_{0,*} \otimes \mathbf{I}_m - (\mathbf{R}_{0,*}^\top \Lambda_1 \mathbf{Q}_*^\top \otimes \mathbf{Q}_* \mathbf{R}_{0,*}) \mathbf{K}_{m,\ell} - \mathbf{I}_\ell \otimes (\mathbf{Q}_* \Lambda_1 \mathbf{Q}_*^\top). \end{aligned}$$

Let

$$\mathcal{V}_0 := \{\mathbf{V} : \mathbf{V} = \mathbf{Q}_* \mathbf{R}_{0,*} \mathbf{S}_1 + \mathbf{Q}_\perp \mathbf{S}_2 \text{ with symmetric } \mathbf{S}_1\}. \quad (\text{A.11})$$

For any  $m \times \ell$  matrix  $\mathbf{V} \in \mathcal{V}_0$ , we have

$$\begin{aligned}
D(\mathbf{Q}_* \mathbf{R}_{0,*}) \text{vec}(\mathbf{V}) &= \text{vec}(\mathbf{V} + \overline{\mathbf{P}}\mathbf{V} - \mathbf{V} \mathbf{R}_{0,*}^\top \boldsymbol{\Lambda}_1 \mathbf{R}_{0,*} - \mathbf{Q}_* \mathbf{R}_{0,*} \mathbf{V}^\top \mathbf{Q}_* \boldsymbol{\Lambda}_1 \mathbf{R}_{0,*} - \mathbf{Q}_* \boldsymbol{\Lambda}_1 \mathbf{Q}_*^\top \mathbf{V}) \\
&= \text{vec}(\mathbf{V} + \mathbf{Q}_\perp \boldsymbol{\Lambda}_2 \mathbf{Q}_\perp^\top \mathbf{V} - \mathbf{V} \mathbf{R}_{0,*}^\top \boldsymbol{\Lambda}_1 \mathbf{R}_{0,*} - \mathbf{Q}_* \mathbf{R}_{0,*} \mathbf{V}^\top \mathbf{Q}_* \boldsymbol{\Lambda}_1 \mathbf{R}_{0,*}) \\
&= \text{vec}(\mathbf{Q}_* \mathbf{R}_{0,*} (\mathbf{S}_1 - \mathbf{S}_1 \mathbf{R}_{0,*}^\top \boldsymbol{\Lambda}_1 \mathbf{R}_{0,*} - \mathbf{S}_1^\top \mathbf{R}_{0,*}^\top \boldsymbol{\Lambda}_1 \mathbf{R}_{0,*})) \\
&\quad + \text{vec}(\mathbf{Q}_\perp (\mathbf{S}_2 + \boldsymbol{\Lambda}_2 \mathbf{S}_2 - \mathbf{S}_2 \mathbf{R}_{0,*}^\top \boldsymbol{\Lambda}_1 \mathbf{R}_{0,*})).
\end{aligned}$$

(iii) Then,

$$\begin{aligned}
\|D(\mathbf{Q}_* \mathbf{R}_{0,*}) \text{vec}(\mathbf{V})\|_2^2 &= \|\mathbf{Q}_* \mathbf{R}_{0,*} (\mathbf{S}_1 - 2\mathbf{S}_1 \mathbf{R}_{0,*}^\top \boldsymbol{\Lambda}_1 \mathbf{R}_{0,*}) + \mathbf{Q}_\perp (\mathbf{S}_2 + \boldsymbol{\Lambda}_2 \mathbf{S}_2 - \mathbf{S}_2 \mathbf{R}_{0,*}^\top \boldsymbol{\Lambda}_1 \mathbf{R}_{0,*})\|_F^2 \\
&= \|\mathbf{S}_1 - 2\mathbf{S}_1 \mathbf{R}_{0,*}^\top \boldsymbol{\Lambda}_1 \mathbf{R}_{0,*}\|_F^2 + \|\mathbf{S}_2 + \boldsymbol{\Lambda}_2 \mathbf{S}_2 - \mathbf{S}_2 \mathbf{R}_{0,*}^\top \boldsymbol{\Lambda}_1 \mathbf{R}_{0,*}\|_F^2 \\
&\leq (1 - 2\lambda_\ell)^2 \|\mathbf{S}_1\|_F^2 + (1 - \lambda_\ell + \lambda_{\ell+1})^2 \|\mathbf{S}_2\|_F^2 \\
&\leq \beta \|\mathbf{S}_1\|_F^2 + \beta \|\mathbf{S}_2\|_F^2 = \beta \|\text{vec}(\mathbf{V})\|_2^2,
\end{aligned}$$

where  $\beta = \max\{(1 - 2\lambda_\ell)^2, (1 - \lambda_\ell + \lambda_{\ell+1})^2\} < 1$ . Let  $\alpha = \frac{1+\beta}{2}$ . By continuity of  $\mathbf{D}$ , there exists an  $\varepsilon \in (0, \varepsilon_0)$  such that  $\|\mathbf{D}(\mathbf{M})\text{vec}(\mathbf{V})\|_2^2 \leq \alpha \|\text{vec}(\mathbf{V})\|_2^2$  for any  $\mathbf{M} \in \mathcal{B}_\varepsilon(\mathbf{Q}_* \mathbf{R}_{0,*})$ , where  $\mathcal{B}_\varepsilon(\mathbf{Q}_* \mathbf{R}_{0,*})$  is an  $\varepsilon$ -open ball in Euclidean space, and for any  $\mathbf{V} \in \mathcal{V}_0$ . The selection of  $\varepsilon$  can be made independent of  $\mathbf{R}_{0,*}$  due to the fact that the underlying matrix Stiefel manifold is compact and it can be covered by finitely many  $\varepsilon$ -ball for any given  $\varepsilon$ .

(iv) Consider a path connecting  $\mathbf{Q}_* \mathbf{R}_{0,*}$  and  $\mathbf{Q}_0$ :

$$\mathbf{M}(\tau) = \tau(\mathbf{Q}_* \mathbf{R}_{0,*} \mathbf{C}_1 + \mathbf{Q}_\perp \mathbf{C}_2) + (1 - \tau)\mathbf{Q}_* \mathbf{R}_{0,*},$$

which is the line segment between  $\mathbf{Q}_0$  and  $\mathbf{Q}_* \mathbf{R}_{0,*}$  with  $\mathbf{M}(1) = \mathbf{Q}_0$  and  $\mathbf{M}(0) = \mathbf{Q}_* \mathbf{R}_{0,*}$ . We have  $\mathbf{M}'(\tau) = \mathbf{Q}_* \mathbf{R}_{0,*} \mathbf{C}_1 - \mathbf{Q}_* \mathbf{R}_{0,*} + \mathbf{Q}_\perp \mathbf{C}_2 \in \mathcal{V}_0$ . By Mean Value Theorem on this curve,

$$\begin{aligned}
\|\text{vec}(\mathbf{Q}_1) - \text{vec}(\mathbf{Q}_* \mathbf{R}_{0,*})\|_2 &= \|\text{vec}(g(\mathbf{M}(1))) - \text{vec}(g(\mathbf{M}(0)))\|_2 \\
&\leq \sup_{\tau \in [0,1]} \|D_{\mathbf{M}(\tau)} \text{vec}(\mathbf{M}'(\tau))\|_2 \leq \sqrt{\alpha} \|\text{vec}(\mathbf{Q}_0) - \text{vec}(\mathbf{Q}_* \mathbf{R}_{0,*})\|_2.
\end{aligned}$$

(v) We can define  $\mathbf{R}_{1,*}$  in a similar way as how  $\mathbf{R}_{0,*}$  is defined:

$$\mathbf{R}_{1,*} := \underset{\mathbf{R} \in \mathcal{S}_{\ell,\ell}}{\text{argmin}} \|\mathbf{Q}_1 - \mathbf{Q}_* \mathbf{R}\|_F. \quad (\text{A.12})$$

Note that  $\mathbf{Q}_1$  is closer to  $\mathbf{Q}_* \mathbf{R}_{1,*}$  than to  $\mathbf{Q}_* \mathbf{R}_{0,*}$ . Then,

$$\|\text{vec}(\mathbf{Q}_1) - \text{vec}(\mathbf{Q}_* \mathbf{R}_{1,*})\|_2 \leq \|\text{vec}(\mathbf{Q}_1) - \text{vec}(\mathbf{Q}_* \mathbf{R}_{0,*})\|_2 \leq \sqrt{\alpha} \|\text{vec}(\mathbf{Q}_0) - \text{vec}(\mathbf{Q}_* \mathbf{R}_{0,*})\|_2.$$

(vi) Furthermore, we can write  $\mathbf{Q}_1$  as  $\mathbf{Q}_1 = \mathbf{Q}_* \mathbf{R}_0 \mathbf{C}_{1,1} + \mathbf{Q}_\perp \mathbf{C}_{1,2}$ , where  $\mathbf{C}_{1,1} \in \mathbb{R}^{\ell \times \ell}$ ,  $\mathbf{C}_{1,2} \in \mathbb{R}^{(m-\ell) \times \ell}$  and  $\mathbf{C}_{1,1}^\top \mathbf{C}_{1,1} + \mathbf{C}_{1,2}^\top \mathbf{C}_{1,2} = \mathbf{I}_\ell$ . Following the same arguments for  $\mathbf{R}_{0,*}$ , we have  $\mathbf{R}_{1,*}^\top \mathbf{R}_0 \mathbf{C}_{1,1}$  is symmetric. That is,  $\mathbf{Q}_1$  can be expressed as  $\mathbf{Q}_1 = \mathbf{Q}_* \mathbf{R}_{1,*} (\mathbf{R}_{1,*}^\top \mathbf{R}_0 \mathbf{C}_{1,1}) + \mathbf{Q}_\perp \mathbf{C}_{1,2}$ . By similar arguments as in (iii)-(iv), we now work on  $D(\mathbf{Q}_* \mathbf{R}_{1,*})\text{vec}(\mathbf{V})$ , where  $\mathbf{V} \in \mathcal{V}_1 := \{\mathbf{V} : \mathbf{V} = \mathbf{Q}_* \mathbf{R}_{1,*} \mathbf{S}_1 + \mathbf{Q}_\perp \mathbf{S}_2 \text{ with symmetric } \mathbf{S}_1\}$ , and similar derivations lead to

$$\|\text{vec}(\mathbf{Q}_2) - \text{vec}(\mathbf{Q}_* \mathbf{R}_{2,*})\|_2 \leq \sqrt{\alpha} \|\text{vec}(\mathbf{Q}_1) - \text{vec}(\mathbf{Q}_* \mathbf{R}_{1,*})\|_2.$$

Iteratively, we have

$$\begin{aligned} & \|\text{vec}(\mathbf{Q}_{t+1}) - \text{vec}(\mathbf{Q}_* \mathbf{R}_{t+1,*})\|_2 \leq \sqrt{\alpha} \|\text{vec}(\mathbf{Q}_t) - \text{vec}(\mathbf{Q}_* \mathbf{R}_{t,*})\|_2 \\ & \leq \alpha^{\frac{t+1}{2}} \|\text{vec}(\mathbf{Q}_0) - \text{vec}(\mathbf{Q}_* \mathbf{R}_{0,*})\|_2. \end{aligned}$$

(vii) Therefore,  $\|\text{vec}(\mathbf{Q}_t) - \text{vec}(\mathbf{Q}_* \mathbf{R}_{t,*})\|_2$  converges to 0. This implies that  $\mathbf{Q}_t \mathbf{Q}_t^\top$  converges to  $\mathbf{Q}_* \mathbf{R}_{t,*} \mathbf{R}_{t,*}^\top \mathbf{Q}_*^\top = \mathbf{Q}_* \mathbf{Q}_*^\top$ , which is independent of  $t$ . It further implies that  $\mathbf{X}(\mathbf{Q}_t)$  converges to  $\mathbf{0}$ , and then  $\mathbf{C}(\mathbf{Q}_t)$  to  $\mathbf{I}_\ell$ . Finally, this leads to the convergence of  $\mathbf{Q}_t$ .  $\square$

**A.9. Proof of Lemma 4.2 and Theorem 4.3.** Proof of Lemma 4.2 is given below. For  $\mathbf{Q} \in \mathcal{S}_{m,\ell}$ , we have  $\|\mathbf{U}\mathbf{\Lambda}\mathbf{U}^\top - \mathbf{Q}\mathbf{Q}^\top\|_F^2 = \|\mathbf{\Lambda} - \mathbf{U}^\top \mathbf{Q}\mathbf{Q}^\top \mathbf{U}\|_F^2$ . Because  $\mathbf{U}^\top \mathbf{Q} \in \mathcal{S}_{m,\ell}$ ,  $\mathbf{U}^\top \mathbf{Q}\mathbf{Q}^\top \mathbf{U}$  is a rank- $\ell$  projection matrix. The best rank- $\ell$  projection matrix to approximate  $\mathbf{\Lambda}$  is  $\mathbf{U}^\top \mathbf{Q}_{\text{opt}} \mathbf{Q}_{\text{opt}}^\top \mathbf{U} = \begin{bmatrix} \mathbf{I}_\ell & \mathbf{0} \\ \mathbf{0} & \mathbf{0} \end{bmatrix}$ . This fact suggests that  $\mathbf{Q}_{\text{opt}} \mathbf{Q}_{\text{opt}}^\top = \mathbf{U}_\ell \mathbf{U}_\ell^\top$ .

Proof of Theorem 4.3 is given below. (a) From Theorem 4.1, we know that  $\bar{\mathbf{P}} = \frac{1}{N} \sum_{i=1}^N \mathbf{Q}_{[i]} \mathbf{Q}_{[i]}^\top$  converges to  $\mathbf{U}\mathbf{\Lambda}\mathbf{U}^\top$  with probability one. By Theorem 2.2 and Lemma 4.2, we have that  $\bar{\mathbf{Q}} \bar{\mathbf{Q}}^\top$  converges to  $\mathbf{U}_\ell \mathbf{U}_\ell^\top$  with probability one. (b) Because  $\bar{\mathbf{Q}} \bar{\mathbf{Q}}^\top \rightarrow \mathbf{U}_\ell \mathbf{U}_\ell^\top$  with probability one, we have  $\bar{\mathbf{Q}} \bar{\mathbf{Q}}^\top \mathbf{A} \rightarrow \mathbf{U}_\ell \mathbf{U}_\ell^\top \mathbf{A} = \mathbf{U}_\ell \mathbf{\Sigma}_\ell \mathbf{V}_\ell^\top$  with probability one. Note that  $\bar{\mathbf{Q}}^\top \mathbf{A} = \widehat{\mathbf{W}}_\ell \widehat{\mathbf{\Sigma}}_\ell \widehat{\mathbf{V}}_\ell^\top$ , and  $\bar{\mathbf{Q}} \bar{\mathbf{Q}}^\top \mathbf{A} = \bar{\mathbf{Q}} \widehat{\mathbf{W}}_\ell \widehat{\mathbf{\Sigma}}_\ell \widehat{\mathbf{V}}_\ell^\top = \widehat{\mathbf{U}}_\ell \widehat{\mathbf{\Sigma}}_\ell \widehat{\mathbf{V}}_\ell^\top$ . Specifically, we have  $\widehat{\mathbf{U}}_\ell \widehat{\mathbf{\Sigma}}_\ell \widehat{\mathbf{V}}_\ell^\top \rightarrow \mathbf{U}_\ell \mathbf{\Sigma}_\ell \mathbf{V}_\ell^\top$  with probability one. By the continuity of left singular vectors as functions of the matrix  $\mathbf{A}$ , which has distinct leading  $\ell$  singular values, we have that  $\widehat{\mathbf{u}}_j$  converges with probability one to  $\mathbf{u}_j$  up to a sign change. Specifically,  $|\widehat{\mathbf{u}}_j^\top \mathbf{u}_j| \rightarrow 1$ .

**A.10. Proof of Theorem 4.5.** Denote  $\widehat{\mathbf{u}}_j$  as  $\widehat{\mathbf{u}}_j = h_j(\frac{1}{N} \sum_{i=1}^N \mathbf{Q}_{[i]} \mathbf{Q}_{[i]}^\top)$ . Then, by SLLN

$$\mathbf{u}_j = \lim_{N \rightarrow \infty} h_j\left(\frac{1}{N} \sum_{i=1}^N \mathbf{Q}_{[i]} \mathbf{Q}_{[i]}^\top\right) = h_j\left(\lim_{N \rightarrow \infty} \frac{1}{N} \sum_{i=1}^N \mathbf{Q}_{[i]} \mathbf{Q}_{[i]}^\top\right) = h_j(\mathbf{U}\mathbf{\Lambda}\mathbf{U}^\top).$$

To apply the delta-method, we need to compute the derivative  $\mathbf{\Delta}_j$ . Let  $\mathbf{M} := \mathbf{U}\mathbf{\Lambda}\mathbf{U}^\top$ . Since  $\mathbf{u}_j$  is the  $j$ th eigenvector, we have  $\mathbf{M}\mathbf{u}_j = \lambda_j \mathbf{u}_j$ , where  $\mathbf{u}_j^\top \mathbf{u}_j = 1$ . Let  $\dot{\mathbf{M}}$  denote a small perturbation to  $\mathbf{M}$ , and  $\dot{\mathbf{u}}_j$  and  $\dot{\lambda}_j$  be corresponding perturbations. Consider small perturbations to both sides of the equation above. Then,

$$\dot{\mathbf{M}}\mathbf{u}_j + \mathbf{M}\dot{\mathbf{u}}_j = \dot{\lambda}_j \mathbf{u}_j + \lambda_j \dot{\mathbf{u}}_j, \quad \text{where } \mathbf{u}_j^\top \dot{\mathbf{u}}_j = 0.$$

Rearrange the equation above, and we have

$$(\lambda_j \mathbf{I}_m - \mathbf{M}) \dot{\mathbf{u}}_j = \dot{\mathbf{M}}\mathbf{u}_j - \dot{\lambda}_j \mathbf{u}_j. \quad (\text{A.13})$$

Let  $(\lambda_j \mathbf{I}_m - \mathbf{M})^+$  be the Moore-Penrose pseudo inverse. Multiply it to both sides of Equation (A.13), we have  $\dot{\mathbf{u}}_j = (\lambda_j \mathbf{I}_m - \mathbf{M})^+ \left( \dot{\mathbf{M}}\mathbf{u}_j - \dot{\lambda}_j \mathbf{u}_j \right) = (\lambda_j \mathbf{I}_m - \mathbf{M})^+ \dot{\mathbf{M}}\mathbf{u}_j$ . Then,  $\dot{\mathbf{u}}_j = [\mathbf{u}_j^\top \otimes (\lambda_j \mathbf{I}_m - \mathbf{M})^+] \text{vec}(\dot{\mathbf{M}})$ . Therefore,

$$\mathbf{\Delta}_j = \frac{\partial \mathbf{u}_j}{\partial \text{vec}(\mathbf{M})^\top} = \mathbf{u}_j^\top \otimes (\lambda_j \mathbf{I}_m - \mathbf{M})^+ = \mathbf{u}_j^\top \otimes (\lambda_j \mathbf{I}_m - \mathbf{U}\mathbf{\Lambda}\mathbf{U}^\top)^+. \quad (\text{A.14})$$

The asymptotic normality can be obtained by a straightforward application of the delta-method.